JGR Atmospheres

RESEARCH ARTICLE
10.1029/2021JD035539

Key Points:

- Both frequency and intensity of extreme precipitation are increasing with spatial variation and it is going to increase further in future
- In general, change in the characteristics of precipitation extremes is dominated by increase in frequency rather than intensity
- High precipitation regions experience an increase in frequency and low precipitation regions experience an increase in intensity

Supporting Information:

Supporting Information may be found in the online version of this article.

Correspondence to:

R. Maity,
rajib@civil.iitkgp.ac.in;
rajibmaity@gmail.com

Citation:

Sarkar, S., & Maity, R. (2022). Future characteristics of extreme precipitation indicate the dominance of frequency over intensity: A multi-model assessment from CMIP6 across India. *Journal of Geophysical Research: Atmospheres*, *127*, e2021JD035539. https://doi.org/10.1029/2021JD035539

Received 7 JUL 2021
Accepted 2 AUG 2022

Author Contributions:

Conceptualization: Rajib Maity
Formal analysis: Subharthi Sarkar
Funding acquisition: Rajib Maity
Investigation: Rajib Maity
Methodology: Subharthi Sarkar, Rajib Maity
Supervision: Rajib Maity
Writing – original draft: Subharthi Sarkar
Writing – review & editing: Rajib Maity

Future Characteristics of Extreme Precipitation Indicate the Dominance of Frequency Over Intensity: A Multi-Model Assessment From CMIP6 Across India

Subharthi Sarkar[1] and Rajib Maity[1]

[1]Department of Civil Engineering, Indian Institute of Technology Kharagpur, Kharagpur, India

Abstract This study presents a comprehensive analysis on the past and future changes in precipitation extremes and quantifies the relative contributions from its frequency and intensity across India, considering five extremeness levels, denoted by 95th, 99th, 99.9th, 99.95th, and 99.97th percentile. Gridded station-based observations from the historical period (1951–2020) and simulations from 14 General Circulation Models for the future (2021–2100), participating in the Coupled Model Intercomparison Project phase 6 (CMIP6) are considered. Apart from an overall increasing pattern of precipitation extremes, it is noticed that the contribution of frequency dominates over intensity. Specifically, the frequency of 99th percentile daily rainfall is projected to increase approximately by two- (SSP245) to three- (SSP585) times in future. We also proposed a new zoning of entire Indian mainland, identified as six Homogeneous Precipitation Zones (HPZs). HPZ-wise analysis reveals that the increase in frequency dominates over intensity for all the HPZs with a varying extent. For instance, increase in frequency is more for the climatologically high-precipitation zones (HPZ-3: Western Ghats, and HPZ-6: North-east India), whereas increase in intensity is more for the low-precipitation zones (HPZ-1: North-west India, and HPZ-4: Peninsular India). The degree of increase gets even more pronounced under the worst scenario SSP585, indicating a potential impact of anthropogenic activities on changing precipitation extremes. Findings of this study should be accounted in the climate change adaptation and mitigation strategies for future.

Plain Language Summary There are different characteristics of extreme precipitation, such as how frequent they occur, its intensity. Owing to change in climate, these characteristics are changing as time passes, as well as from one location to another location. How has it been changed in the past and how will it be changing in future? Is there any link with the nature of rainfall in a region? These are the focus of this study. We considered entire Indian mainland as our study domain that spans across a wide range of climatology. Overall, it is noted that both frequency and intensity are increasing and it is going to increase further in future. Moreover, frequency is increasing more rapidly than intensity. However, this finding varies from region to region. The regions that receive high precipitation, in general, may experience maximum increase in frequency (northeast and western ghats region in India), whereas the regions with relatively low precipitation may experience maximum increase in intensity (southern peninsular India). Such findings are expected to be useful in many applications related to climate change impacts on water sector.

1. Introduction

The intensification of the global hydrological cycle is the most consistent and ubiquitous signature of the changing scenario of climate in this 21st century's world (Allen & Ingram, 2002; Madakumbura et al., 2019; Trenberth, 2011; Trenberth et al., 2003). Consequently, the regime of precipitation has altered worldwide significantly, manifesting itself in terms of changes in both intensity and frequency (Giorgi et al., 2011, 2014; Madakumbura et al., 2019; Trenberth et al., 2003). Interestingly, the mean precipitation has not altered much due to global warming, being restricted mainly by energy constraints on the global scale (Allen & Ingram, 2002; O'Gorman et al., 2012; Pendergrass & Hartmann, 2014). However, it has caused a significant redistribution of extreme precipitation all over the world (Papalexiou & Montanari, 2019; Sarkar & Maity, 2021). Several studies in the recent past have evidently confirmed a strong association between the increasing precipitation extremes and global warming, that is, increase in global mean surface temperature (Berg et al., 2013; Fischer & Knutti, 2016; Ghosh et al., 2012; Hennessy et al., 1997; Kharin et al., 2013; Mishra et al., 2012; X. Zhou et al., 2018), which results in increased atmospheric moisture-holding capacity and subsequently causes intensification of the hydro-

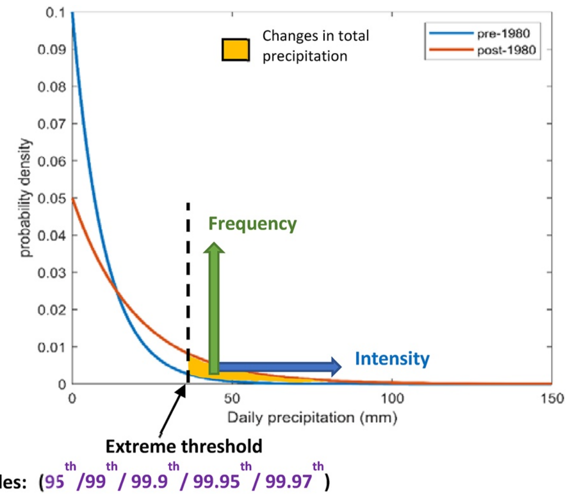

Figure 1. Schematic illustration of the probability density function (pdf) of daily precipitation at some randomly selected grid-point over India for Pre-1980 and post-1980 period.

logical cycle (Jacob & Hagemann, 2007; Sharma & Mujumdar, 2019). Although the complete physical understanding of the association between precipitation extremes and global warming is still developing (Myhre et al., 2019), there is a general agreement within the literature that the nature of extreme precipitation is changing with time. Hence, a proper systematic analysis of changing spatiotemporal patterns of precipitation extremes has become indispensable, considering its significant socio-economic impacts through flooding, crop damages, erosion, health hazard, water contamination issues, etc. (Guhathakurta et al., 2011; Mukherjee et al., 2018; Pall et al., 2011; Papalexiou & Montanari, 2019; Rajeevan et al., 2008).

The warming-induced changes in extreme precipitation are characterized by the changes in its two attributes—frequency and intensity, in four possible ways: more frequent and more intense events, more frequent and less intense events, less frequent and more intense events, or less frequent and less intense rainfall events (Madakumbura et al., 2019). Hence, the contribution from both frequency and intensity, either jointly or individually, are to be considered to understand the overall changing characteristics of extreme precipitation. To understand the contribution of frequency and intensity toward changes in total extreme precipitation, a schematic diagram of the probability density function (pdf) of daily precipitation is shown in Figure 1 for a random grid point in India (See Section 2). The blue and red curves designate the pdfs of daily precipitation for the reference period (here, pre-1980 period i.e., 1951–1980) and the period of interest (here post-1980 period i.e., 1981–2020), respectively. From the shift in pdf, the difference in response of the light rainfall and heavy rainfall events responds to the warming scenario between pre- and post-1980 is realized; the wetter events become more frequent at the cost of light or no precipitation days (Fischer & Knutti, 2016). Now, one extreme threshold is defined as shown in the black dashed line in Figure 1, and the area enclosed between those two pdfs (the yellow area) indicates the total change in extreme precipitation above that particular threshold. Two main components of this change are shown in the figure—(a) the blue horizontal line indicating the changes in intensity, and (b) the green vertical line indicating the changes in frequency. Thus, both frequency and intensity contribute together toward the total change in extreme precipitation.

The intensity of extreme rainfall, that is, the magnitude of heavy rainfall (above some pre-defined threshold) per unit time (e.g., day) has been reported to increase by many global and regional studies based on observations and/or model simulations (Allan et al., 2014; Allen & Ingram, 2002; Berg et al., 2013; Fischer & Knutti, 2016; Kharin et al., 2013; O'Gorman, 2015; Sarkar & Maity, 2020b; Sillmann et al., 2013). On the other hand, the likely changes in the frequency of extreme precipitation, that is, the number of events above some pre-defined threshold per unit time, have not been explored in detail (Barbero et al., 2017; Myhre et al., 2019; Villarini et al., 2013), barring few recent studies in some parts of the world, for example, Europe (Myhre et al., 2019; Papalexiou & Montanari, 2019), United States (Stegall & Kunkel, 2019), Japan (Myhre et al., 2019), China (Deng et al., 2018; Lu et al., 2014) etc. Changes in both these components of extreme precipitation are very important to various hydrologic designs and applications (Kao & Ganguly, 2011). For example, the Intensity-Duration-Frequency (IDF) curve, which is most commonly used for planning and designing various hydrologic infrastructures, traditionally assumes stationarity in the rainfall data. So, the existing infrastructures will expose to higher risk due to the expected increase in intensity and frequency of extreme precipitation under future changing scenarios of climate. Therefore, the planning and design of such structures need to be strategically updated in the context of climate change. Here lies the motivation behind this study.

The objective of this study is to analyze the future possible changes (if any) in the total amount of extreme precipitation and quantify the contributions from changes in intensity and changes in frequency. Toward this, the entire Indian mainland is considered as the study area, which is also considered as a climate "hot-spot," characterized by a high density of vulnerable population and a strong signal of climate change in the recent past (De Souza et al., 2015). In the last couple of decades, India has faced several catastrophes related to extreme rainfall, causing large damage to infrastructures and affecting millions of lives (Mukherjee et al., 2018). Thus, a comprehensive spatiotemporal analysis will be immensely useful for the assessment of the changes in precipitation extremes at different levels of "rareness" (or "extremeness") and quantification of the relative contributions from the changes in frequency and intensity. Moreover, to assess the spatial variation of the changes in extreme precipitation across different climate regimes, a new zoning is proposed for the study area—that forms another objective of this study. This new zoning across India identifies six Homogeneous Precipitation Zones (HPZs), by coupling two important characteristics of precipitation, viz., mean annual precipitation and seasonality. Following this, the final objective of this study is to analyze the observed and future-projected changes in precipitation extremes at the pan India level, as well as zonal level, across these six HPZs. Gridded observations are used to evaluate the observed changes in the past, and simulations from 14 state-of-the-art General Circulation Models (GCMs) are used to project the future-possible changes.

The remaining portion of this paper is organized as follows. Details on the observed rainfall data and future modeled rainfall data are provided in Section 2. Following this, the methodology adopted in this study is explained in Section 3. A detailed discussion on the results, that is, observed and future-projected changes in precipitation extremes over India, is presented in Section 4. Finally, the conclusions of the study are provided in Section 5.

2. Data Used

2.1. Observed Rainfall Data

The daily gridded observed rainfall data is obtained from the India Meteorological Department (IMD) for the period 1951–2020 (Pai et al., 2014). This data set of 0.25° latitude × 0.25° longitude resolution was developed using observed records of daily rainfall data from 6,995 rain-gauge stations across India. This gridded precipitation data set from IMD has been successfully used for various hydroclimatic studies in recent times (S. Dash & Maity, 2019; Mishra, 2020; Mishra et al., 2020; Sarkar & Maity, 2020a; Suman & Maity, 2020). The entire 70 years of data is split into two parts, viz. Pre-1980 period (1951–1980) and Post-1980 (1981–2020) to capture the changes (if any) in precipitation extremes. The year 1980 is chosen as the transition year as several earlier studies have detected some abrupt, substantial, and persistent changes or "shift" in the state of natural climatic systems around the mid- to late- 1970s in different parts of the globe, as well as in India (H. Chen et al., 2019; Dai et al., 2018; S. Dash & Maity, 2019; Reid et al., 2016; Sabeerali et al., 2012; Sarkar & Maity, 2020a; T. Zhou et al., 2009). This phenomenon is generally referred as "global shift in climate regime in 1970s" in literature, and its impact is manifested in several hydroclimatic variables, such as temperature, air pressure, wind field, precipitation etc. Hence, a comparative analysis between the pre- and post-1980 period by choosing the year 1980 as the change year is expected to capture the potential impact of this 'global shift in climate regime in 1970s' on precipitation extremes over India.

2.2. Simulated Future Precipitation Data

For future analysis, the simulated daily precipitation datasets (2021–2100) following two Shared Socioeconomic Pathways (SSPs), viz., SSP245 and SSP585 are obtained from 14 state-of-the-art GCMs (see Table 1) that participated in the Coupled Model Intercomparison Project-6 (CMIP6) (URL: https://esgf-node.llnl.gov/search/cmip6/ accessed in May 2021). The selection of these 14 GCMs from CMIP6 was based on their availability under r1i1p1f1 initial condition and three scenarios—historical, SSP245 and SSP585, at the time of initiation of this study. In general, CMIP provides a fundamental basis for coordinated climate research on the international level, as contributed from several climate modeling centers (Eyring et al., 2016). The present study considers the most recent version of CMIP, that is, CMIP6, which undergoes substantial improvements over its earlier versions (such as CMIP3, CMIP5) in multiple aspects, such as finer horizontal resolution, improved parameterizations of cloud microphysics, better representation of the synoptic processes, and better agreement with the global energy balance (Supharatid et al., 2021). Thus, more reasonable and reliable projections can be obtained from CMIP6 outputs as compared to its previous versions (C. A. Chen et al., 2021; Di Luca et al., 2020; Li et al., 2021; Wang et al., 2021) at global, as well as regional scale—which the present study explores.

Total of 80 years of future GCM data (2021–2100) is equally divided into two parts, viz., near-future period (2021–2060) and far-future period (2061–2100), to capture the temporal change in the characteristics of precipitation extremes in upcoming years of the present century w.r.t. the base-period (1981–2010). The historical simulations are obtained for the base-period (1981–2010), along with future simulations following SSP245 and SSP585, to understand two possible future scenarios of changes in extremes with respect to the historical reference. For instance, SSP585 is the most pessimistic scenario with strong economic growth, rapid technological advances, integrated global market, but at the cost of exploiting the abundant fossil fuel resources (Gidden et al., 2019). No suitable climate policy and consequent high anthropogenic release of greenhouse gases lead to a target radiative forcing of 8.5 W/m^2 by 2100 in SSP585. On the other hand, SSP245 depicts a "middle of the road" scenario with moderate population growth, uneven development and income growth across countries, and having a target radiative forcing of 4.5 W/m^2 at the end of the century. Thus, by comparing changes between SSP585 and SSP245, the possible impact of higher anthropogenic activity and greenhouse gas emissions can be assessed.

3. Methodology

3.1. Background

India is a vast country with spatially diverse precipitation characteristics. On one side, it has the world's wettest place, Mawsynram (receiving over 5,000 mm rainfall a year); on the other side, it has Thar Desert (less than 200 mm rainfall a year). The monsoon pattern is also different in different parts of the country; where most places are dominated by the south-west monsoon, few places are also influenced by the north-east monsoon. So, just an overall pan-India analysis may not capture the complete picture of changing precipitation extremes. Rather a zone-level analysis, identifying the places with uniform or coherent precipitation characteristics would be more meaningful. Toward this, the IMD recommends the use of Homogeneous Monsoon Region (HMR), which was first developed by Parthasarathy et al. (1996). Lately, few other zoning patterns have also been proposed/used in some studies (Bhatla et al., 2019; Saikranthi et al., 2013), however, the HMRs proposed by IMD are used in various hydroclimatic studies across India (S. K. Dash et al., 2002; Rajendran et al., 2013; Sharma & Mujumdar, 2017; Zheng et al., 2016). Parthasarathy et al. (1996) proposed this zoning by grouping then 29 meteorological sub-divisions of India into five HMRs, mainly on the basis of monsoon precipitation characteristics. However, this proposition of HMRs has always been questionable for various reasons. Firstly, those 29 sub-divisions—on the basis of which the HMRs were developed, were proposed by IMD around mid of the last century after an exhaustive compilation of various rainfall-statistics. However, for the practical convenience (such as issuing weather warnings to government functionaries, informing the general public), these sub-divisional boundaries were always made to conform some administrative jurisdictions. Eventually, the developed HMRs also follow the inter-state political boundaries—which can be dubious from the climatological point of view. As a critical example, this existing zoning of HMRs cannot differentiate the windward side of the Western Ghats, which receives a much higher amount of precipitation as compared to the west-central or peninsular India (See Figure 3c). Similarly, the entire West Bengal is grouped with north-east India, despite having a considerably different rainfall pattern.

Thus, we argue that the consideration of the existing HMRs may not capture the true scenario of varying precipitation characteristics over India. Hence, here we propose a new zoning for India, namely Homogeneous Precipitation Zones (HPZs), coupling the annual rainfall magnitudes and the seasonality together. Firstly, this new zoning does not only consider the rainfall during monsoon months, rather the rainfall over the entire year is considered. Secondly, the seasonal variation of monthly rainfall is also considered, which is a very important aspect of rainfall, particularly from the Indian perspective. For instance, a place with moderate precipitation, but an even monthly distribution will ensure a consistent and adequate availability of water throughout the year. On the other hand, a place with substantial precipitation, but an uneven monthly distribution will indicate a surplus of water during a particular period of a given year and a deficit during the remaining period in a given year. Therefore, the consideration of seasonal variability of precipitation is extremely important in delineating precipitation zones, particularly under this changing climatic and socio-economic scenario. On one hand, the water demand is increasing due to increased population, urbanization, industrial and agricultural requirements, and on the other hand, the regular spatio-temporal pattern of precipitation is being altered. Keeping all these factors in mind, the newly proposed HPZs is can be considered as a more appropriate zoning for India, in the present context of changing climate. The theoretical background of these HPZs is discussed in detail in the next sub-section.

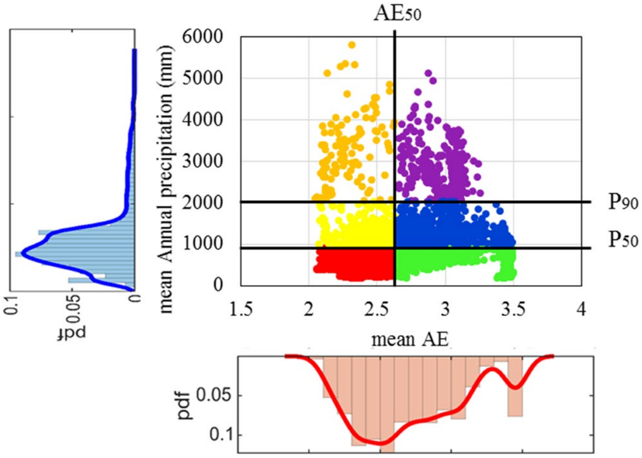

Figure 2. Scatter plot between mean annual precipitation and AE across India using data from 1951 to 1980.

3.2. Proposed Zoning of Indian Mainland: Homogeneous Precipitation Zones (HPZs)

This proposed zoning is done based on the average annual precipitation (P) and seasonal variation of monthly precipitation over the period 1951–1980 with the observational records. To quantify the seasonality, an information theory-based metric named Apportionment Entropy (AE) is utilized, which provides a descriptive non-parametric measure of the seasonal variation for any data (here, monthly precipitation). The value of AE for kth year is calculated by

$$AE_k = -\sum_{i=1}^{12} (p_{ik}/P_k)\log_2(p_{ik}/P_k) \tag{1}$$

where, p_{ik} is the monthly precipitation for ith month in kth year and P_k is the total annual precipitation for the kth year, hence given by $P_k = \sum_{i=1}^{12} p_{ik}$. Theoretically, the magnitude of AE may range between zero and the maximum value of $\log_2 12 (\approx 3.585)$. Higher the magnitude of AE, less seasonal is the precipitation data, and vice versa. Next, the average values of P and AE are calculated for all grid points over the reference period and plotted as a scatter plot. This P versus AE plot is divided into six zones, named Homogeneous Precipitation Zones (HPZs), delineated through some thresholds of P and AE (see Figure 2), further discussed in detail in Section 4. The methodology presented in the following subsection is applied to these zones separately as well as the whole Indian mainland (henceforth, all-India).

3.3. Calculation of Precipitation Extremes and Comparative Analysis

Spatial and temporal changes in precipitation extremes are analyzed for different percentiles of the daily precipitation pdfs across the Indian mainland as well as its six aforementioned HPZs. Five percentile values are considered to define the extreme thresholds, viz., 95th, 99th, 99.9th, 99.95th, and 99.97th. The concept of determining these percentiles is similar to the standard procedure followed by the Expert Team on Climate Change Detection, Monitoring and Indices (ETCCDI). Firstly, the "wet" days, that is, the days with more than 1 mm precipitation are filtered out from the entire daily precipitation time series, and then these percentiles are calculated non-parametrically. Thus, in this procedure, any trace precipitation event (with less than 0.04 mm in a day, as per Indian standard) simulated by the GCMs gets identified as "dry" event. Additionally, the present study considers three rarer thresholds (99.9th, 99.95th, and 99.97th percentile) than the ETCCDI recommendation (95th and 99th percentile) while calculating different extreme precipitation indices. With this background, two different sets of comparative analysis is performed in this study, (a) Observational analysis over the historical period (1951–2020), and (b) Multi-model Analysis on projected changes over the future period (2021–2100). In the case of observational analysis, the percentiles are calculated based on the pre-1980 (1951–1980) IMD-observed data to capture the likely changes in post-1980 (1981–2020) period. In case of future analysis, the percentiles calculated over the base-period 1981–2010 are used as the reference to evaluate temporal changes in the near-future (2021–2060) and far-future (2061–2100) periods.

As mentioned before, the future analysis involves simulated data from 14 different CMIP6-GCMs. In general, the GCM outputs, particularly the simulated precipitation data systematically under- or overestimates the actual observations, and thus possess a substantial amount of bias (Abdelmoaty et al., 2021; Ashfaq et al., 2017; Maity et al., 2019; Mishra et al., 2014). Regardless of several advancements in the latest version of CMIP, that is, CMIP6, such systemic bias is inevitable in future-projected precipitation. Therefore many studies recommend first correcting the bias present in GCM data before using it for any impact assessment studies (Christensen et al., 2008; Kunstmann et al., 2004; Ott et al., 2013). Bias-correction methodologies have a long history in the literature, including techniques, such as linear (Lenderink et al., 2007), non-linear (Leander & Buishand, 2007; Leander et al., 2008), distribution-based quantile mapping (Mao et al., 2015; Pierce et al., 2015), empirical quantile mapping (Piani et al., 2010; Themeßl et al., 2011), copula-based RMPH technique (Maity et al., 2019; Suman et al., 2021) etc. In spite of such developments, bias correction has always been a controversial topic of discussion

Table 1
Basic Details of 14 CMIP6-GCMs Used in This Study

S. No	Model name	Source institute	Actual resolution (latitude × longitude)	Resolution after regridding (latitude × longitude)
1	ACCESS-CM2	Commonwealth Scientific and Industrial Research Organization, Australia	$1.25^{o} \times 1.875^{o}$	$0.25^{o} \times 0.25^{o}$
2	ACCESS-ESM1-5		$1.25^{o} \times 1.875^{o}$	$0.25^{o} \times 0.25^{o}$
3	BCC-CSM2-MR	Beijing Climate Center, China	$1.1121^{o} \times 1.125^{o}$	$0.25^{o} \times 0.25^{o}$
4	CanESM5	Canadian Center for Climate Modeling and Analysis, Canada	$2.7673^{o} \times 2.8125^{o}$	$0.25^{o} \times 0.25^{o}$
5	EC-Earth3	EC-Earth-Consortium	$0.70^{o} \times 0.70^{o}$	$0.25^{o} \times 0.25^{o}$
6	EC-Earth3-Veg		$0.70^{o} \times 0.70^{o}$	$0.25^{o} \times 0.25^{o}$
7	CESM2_WACCM	National Center for Atmospheric Research, USA	$0.9424^{o} \times 1.25^{o}$	$0.25^{o} \times 0.25^{o}$
8	CMCC-CM2-SR5	Fondazione Centro Euro-Mediterraneo sui Cambiamenti Climatici, Italy	$0.9424^{o} \times 1.25^{o}$	$0.25^{o} \times 0.25^{o}$
9	MPI-ESM1-2-HR	Max Planck Institute for Meteorology, Hamburg, Germany	$0.935^{o} \times 0.9375^{o}$	$0.25^{o} \times 0.25^{o}$
10	MPI-ESM1-2-LR		$1.8652^{o} \times 1.8750^{o}$	$0.25^{o} \times 0.25^{o}$
11	IPSL-CM6A-LR	Institut Pierre Simon Laplace, France	$1.2676^{o} \times 2.5^{o}$	$0.25^{o} \times 0.25^{o}$
12	IITM	Indian Institute of Tropical Meteorology Pune, India	$1.9048^{o} \times 1.8750^{o}$	$0.25^{o} \times 0.25^{o}$
13	INM-CM4-8	Institute for Numerical Mathematics, Russian Academy of Science, Russia	$1.5^{o} \times 2.0^{o}$	$0.25^{o} \times 0.25^{o}$
14	INM-CM5-0		$1.5^{o} \times 2.0^{o}$	$0.25^{o} \times 0.25^{o}$

in the scientific community (Ehret et al., 2012; Knutti et al., 2010; Maraun, 2016). In particular, Maraun (2016) argued that the bias correction of climate model data may lead to superficial and implausible projections due to their misrepresentation of long-term climate trends and variability. Thus, in this study, the projected changes in any precipitation-related statistic/percentile from a GCM over the future period (2021–2100) are determined with respect to the same derived from the simulated historical values (1981–2010) of the same GCM. Thus, we can obtain a relative metric of changes in future for each GCM.

Next, the projected changes are averaged across the GCMs to obtain the multi-model ensemble mean changes over the future. However, from Table 1, it can be observed that all 14 CMIP6-GCMs have different spatial resolutions. Hence, the bilinear interpolation, a standard re-gridding technique, is used to bring all of them down to the same resolution of the observed data from IMD (i.e., 0.25° latitude × 0.25° longitude) to conduct the multi-model analysis. Although, different regridding techniques are commonly used in climate change impact assessment studies (Alexander et al., 2006), its impact on precipitation extremes, irrespective of the technique, cannot be denied (Rajulapati et al., 2021). In Section A1 in Supporting Information S1, a detailed illustrative example is shown on the potential effect of regridding, which reveals an underestimation of precipitation extremes. This degree of underestimation increases with the increase in the rareness of the extremes. However, we argue that, for a certain extreme threshold from a particular GCM, the degree of underestimation due to regridding remain more or less similar for historical, as well as future period (see Figure S1 in Supporting Information S1). Therefore, it may be concluded that the regridding may have some impact on precipitation extremes, but while estimating the relative changes in future with respect to a historical reference period, the effect of regridding may be safely ignored.

Now for each threshold, three attributes of extreme precipitation are calculated over each year to conduct the comparative analysis; Total Precipitation (TP) in mm, Frequency (F) in (year^{-1}), and intensity above the threshold percentile (I) in mm/day. For example, TP99 designates the "Total Precipitation from top 1% heaviest precipitation events," and it is calculated as the summation of daily precipitation magnitudes that exceeds the 99th percentile in a particular year. Next, the average annual TP over the base period and the period of interest are determined for each of the extreme thresholds, as defined earlier, followed by the estimation of the corresponding percentage changes in the period of interest with respect to the base period. It is followed by the evaluation of the contributions from changes in frequency and intensity separately toward the changes in total precipitation above a certain extreme threshold. The changes in frequency is calculated as the change in the number of events per unit time with precipitation above the pre-defined thresholds. The change in intensity is calculated as the average precipitation above the threshold for the strongest equal number of events as noted from the reference period. It

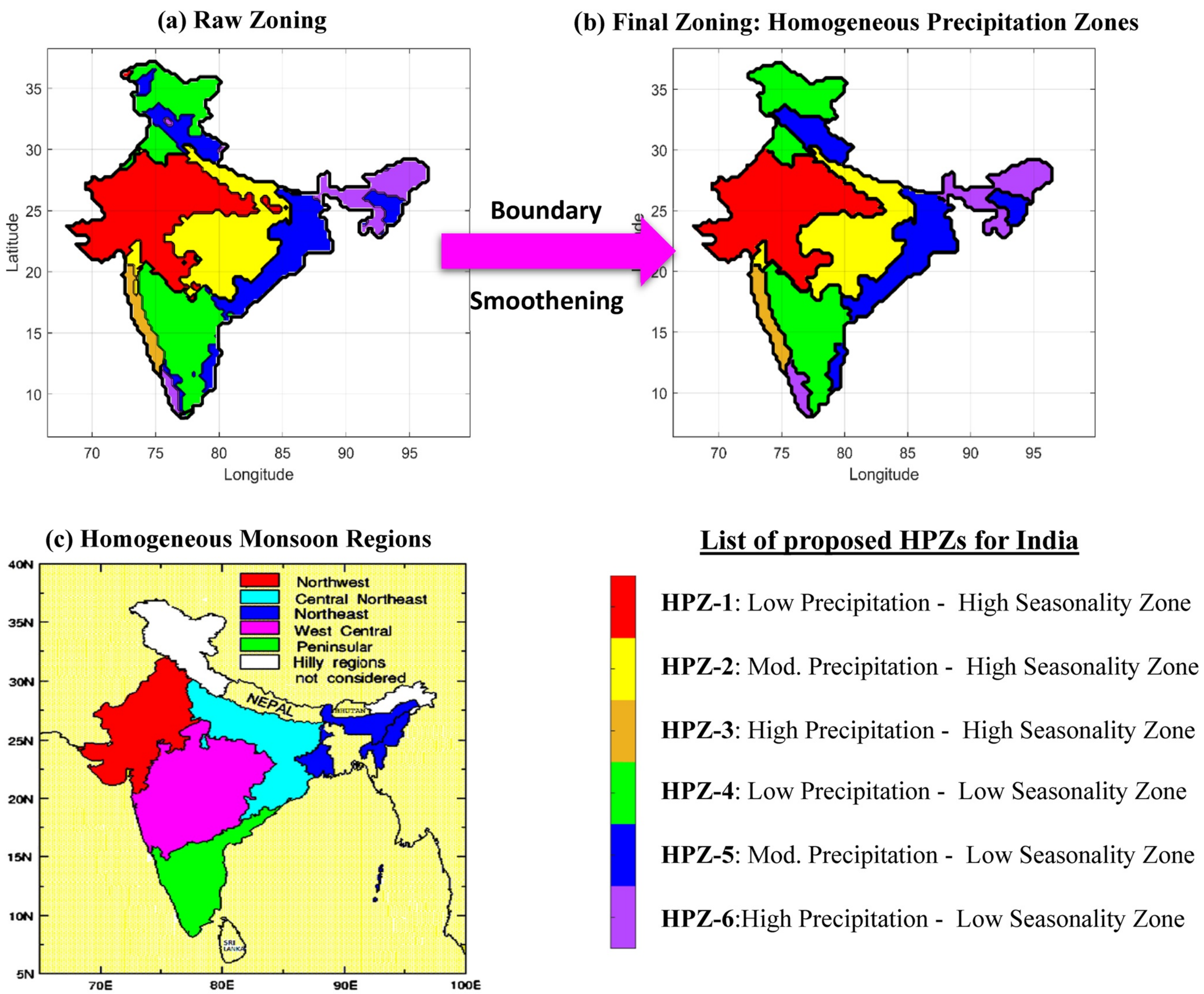

Figure 3. Proposed Homogeneous Precipitation Zones (HPZs) across the Indian mainland, (a) Raw spatial distribution of zones directly obtained from the scatter plot in Figure 2. (b) Final spatial distribution of zones after smoothening the boundaries. (c) The existing Homogeneous Monsoon Regions for India, as developed by Parthasarthy et al. (1996).

must be noted here that, due to diverse spatial variation of extreme precipitation across India, we document the temporal changes in all three attributes (*TP*, *F* and *I*) as percentage changes—a relative metric instead of absolute changes. This helps us to conduct a detailed inter-HPZ comparison as well.

To further clarify the computational approach, let us consider one hypothetical example, where the reference period has 99th percentile value as 100 mm/day, and observes 3 rainfall events above the 99th percentile with values 105, 120, and 125 mm/day, whereas the period of interest has 5 rainfall events that exceed 100 mm/day threshold with values 102, 115, 120, 130, 140 and 145 mm/day. Now to calculate the changes in intensity, we filter out the same number (here 3, as in the reference period) of strongest events from the "period of interest," even if the lowest value is lower than the pre-defined threshold (here, 100 mm/day). So in this example, the 3 strongest events of precipitation in the period of interest are 130, 140, and 145 mm/day. Taking the average of the equal number of strongest precipitation events as 116.67 mm/day (reference period) and 138.33 mm/day (period of interest), an increase of 18.5% in intensity and an increase in frequency from 3 to 5 can be reported in the period of interest. However, it may be noted that, if the period of interest has only 2 events higher than the threshold of 100 mm/day, still the same number, that is, 3 number of strongest events (with one value less than 100 mm/day), is to be considered to estimate the change in intensity in the period of interest.

Table 2
Details of the Uniform Precipitation Zones (HPZs) Proposed in This Study

HPZ number	Criteria for classification	Zone name	Abbreviations
HPZ-1	$P < P_{50}$ and $AE < AE_{50}$	Low precipitation high seasonality	$P_L S_H$
HPZ-2	$P_{50} < P < P_{90}$ and $AE < AE_{50}$	Mod. precipitation high seasonality	$P_M S_H$
HPZ-3	$P > P_{90}$ and $AE < AE_{50}$	High precipitation high seasonality	$P_H S_H$
HPZ-4	$P < P_{50}$ and $AE > AE_{50}$	Low precipitation Low seasonality	$P_L S_L$
HPZ-5	$P_{50} < P < P_{90}$ and $AE > AE_{50}$	Mid precipitation low seasonality	$P_M S_L$
HPZ-6	$P > P_{90}$ and $AE > AE_{50}$	High precipitation low seasonality	$P_H S_L$

4. Results and Discussion

4.1. Homogeneous Precipitation Zones (HPZs)

Gridwise mean annual precipitation (P) and mean AE over the reference period (1951–1980) are plotted as a scatter plot in Figure 2, which is then divided into six different HPZs as shown by different colors. In case of seasonality, only the 50th percentile, that is, AE_{50} is used to differentiate between High-seasonality ($AE < AE_{50}$) and Low-seasonality zones ($AE > AE_{50}$). However, in case of annual precipitation, we also used the 90th percentile to designate three different zones, viz., Low-rainfall ($P < P_{50}$), Moderate-rainfall ($P_{50} < P < P_{90}$), and High-rainfall zones ($P > P_{90}$). Thus, in this classification approach, the characteristics of both annual precipitation magnitude and seasonal variability are combined into six distinct HPZs across the Indian mainland.

The spatial distribution of these HPZs is shown in Figure 3a, where a few small patches of zones within the boundary of another adjoining zone can be noticed in some parts of the country. Such cases are taken care of manually and converted to the zone it is surrounded by to obtain a smoother boundary of zones and to maintain the spatial contiguity of the zones. After performing such manual boundary smoothening, the finalized zones are shown in Figure 3b. This Figure 3b can be considered as the final zoning map for HPZs across the Indian mainland, proposed in this study. Further detailed insight into this zoning is shown in Table 2, including the criterion for classification, zone number, zone full name, and corresponding abbreviations. For a quick comparison, existing HMRs are shown in Figure 3c, which reveals that, unlike the existing HMRs, this newly proposed HPZs (Figure 3b) can successfully identify the windward side of Western Ghats as a distinct zone, that is, HPZ-3 or High Precipitation High Seasonality zone.

On further investigation of Figure 3b, we can see the HPZ-1 or Low Precipitation High Seasonality zone ($P_L S_H$) lies in the north-western part of India, predominantly consisting of Gujrat and Rajasthan, and some portion of western Uttar Pradesh and Madhya Pradesh. The HPZ-2 or Moderate Precipitation High Seasonality zone ($P_M S_H$) can be found in the central part of India, mostly spanning eastern Uttar Pradesh and Madhya Pradesh, and Chhattisgarh. As mentioned earlier, the Western Ghats are identified as HPZ-3 or High Precipitation High Seasonality zone ($P_H S_H$). The HPZ-4 or Low Precipitation Low Seasonality zone ($P_L S_L$) can be observed in two different parts of India; Peninsular India (parts of Maharashtra, Telangana, Karnataka, Southern Andhra Pradesh, and Tamilnadu) and northern India (Punjab, Jammu-Kashmir, and Ladakh portion). The HPZ-5 or Moderate Precipitation Low Seasonality zone ($P_M S_L$) is rather dispersed at multiple places across the Indian mainland; mostly in the eastern part of India (West Bengal, eastern Bihar, Jharkhand, and Odisha), parts of the eastern coast in Southern India (some coastal parts of Andhra Pradesh and Tamilnadu), parts of northern India (Uttarakhand and Himachal Pradesh) and some portion in north-east India. Lastly, the HPZ-6 or High Precipitation Low Seasonality zone ($P_H S_L$) can be mostly found in north-east India and Kerala.

4.2. Observational Changes in Precipitation Extremes

4.2.1. All-India Analysis

Gridded observations are used to analyze the changes in precipitation extremes (TP, F, and I) in the post-1980 period w.r.t pre-1980 period. Figure 4 shows the spatial distribution of changes in TP, F, and I after the transition year 1980 for all five thresholds across the Indian mainland. It is noticed that the majority of the Indian mainland has experienced an increase in precipitation extremes (TP, F, and I) in the post-1980 period. Barring few

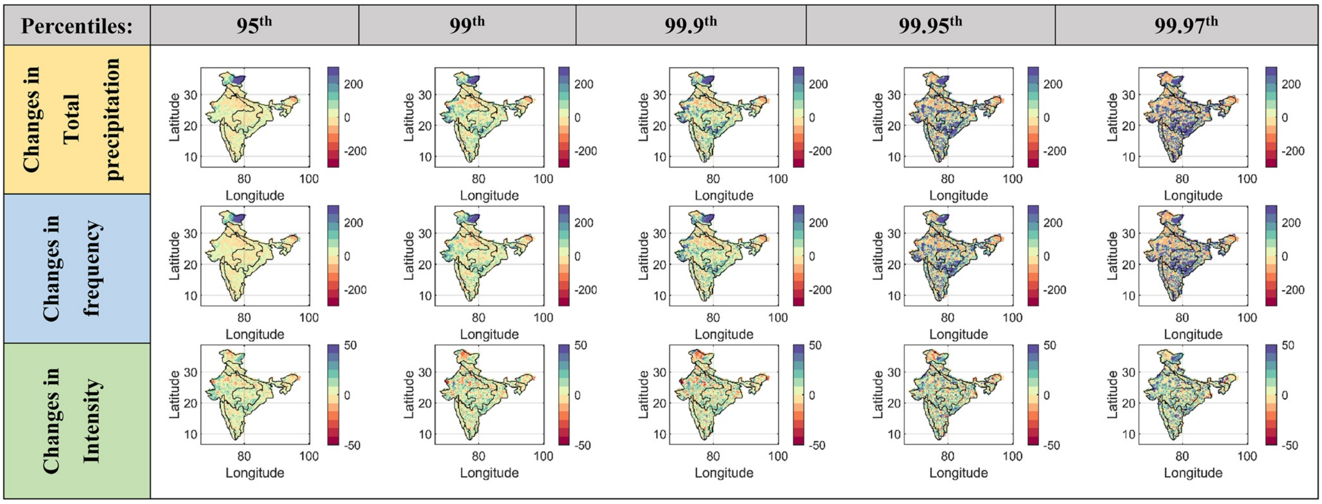

Figure 4. Spatial distribution of observed changes (in percentage) in total precipitation, frequency, and intensity in the post-1980 period (1981–2020) compared to pre-1980 period (1951–1980) across Indian mainland for all five percentiles (95th, 99th, 99.9th, 99.95th, and 99.97th) used in this study.

places in north India (particularly in the Gangetic plain) and north-east India, precipitation extremes are found to increase in most of the places across the Indian mainland, especially in the eastern coastal regions in South India and north-western region (e.g., parts of Gujarat and Rajasthan). Also, the extent of the increase becomes more prominent in those aforementioned places with the increase in "extremeness" of the threshold considered. However, an unusually high level of the increase in extreme precipitation is noticed in the parts of Ladakh, located in the extreme northern tip of India. The reliability of the precipitation data is questionable in that region due to poor networks of rain gauges (Kothawale & Rajeevan, 2017). Hence, this part is excluded while calculating the area-averaged values of changes. Accordingly, the quantitative output of the comparative analysis between the pre- and post-1980 periods is shown as bar plots in Figure 5 and Table 3. Results confirm a general pattern of increasing precipitation extremes across the Indian mainland during the post-1980 period.

From Figure 5 (top row), an interesting feature of the changing pattern of precipitation extremes is noticed. The all-India average changes in *TP*, *F*, and *I*—all increase with the extremeness of the heavy precipitation events. In other words, a strong monotonic increase in total extreme precipitation, its frequency, and intensity is observed with the extremeness of the event (defined by the threshold). For instance, the observed changes in *TP*, *F*, and *I* are approximately 29%, 23%, and 4%, respectively, for the 99th percentile, but these values increases to 163%, 124%, and 12% for the 99.97th percentile. Another important observation is that the increase in frequency is much higher than that of intensity.

This can be further elucidated from Figure 6, which represents the change in total extreme precipitation above the 99th percentile as a combination of changes in intensity and frequency. This scatter plot is divided into four different quadrants with respect to the zero-change lines along both axes, viz., Quadrant-I: increase in both *F* and *I*, Quadrant-II: increase in *F* but decrease in *I*, Quadrant-III: decrease in both *F* and *I*, and Quadrant-IV: decrease in both F but increase I. Firstly we can observe that, most of the grid points are lying in quadrant-I, experiencing increase in both F and I, and hence in the TP. Apart from that, some interesting observations can be made from quadrant-II and quadrant-IV. From quadrant-II, it can be observed that, even after reduction in intensity, the total precipitation has mostly increased (shown by different shades of blue), which can be solely attributed to increase in frequency. On the other hand, in quadrant-IV, due to the reduction in frequency, most of the grid points are experiencing a reduction in total precipitation as well (shown by different shades of red), even though the intensity has increased. These observations evidently show the dominance of frequency changes over the changes in intensity toward changes in total extreme precipitation above a certain threshold. This can be further confirmed by the respective pdfs of frequency changes and intensity changes along both axes. However, the contribution from intensity changes cannot be denied, of course. Though this example is shown for only one extreme threshold, that is, 99th percentile, it holds true for all four remaining thresholds as well. Overall, it is also noticed that

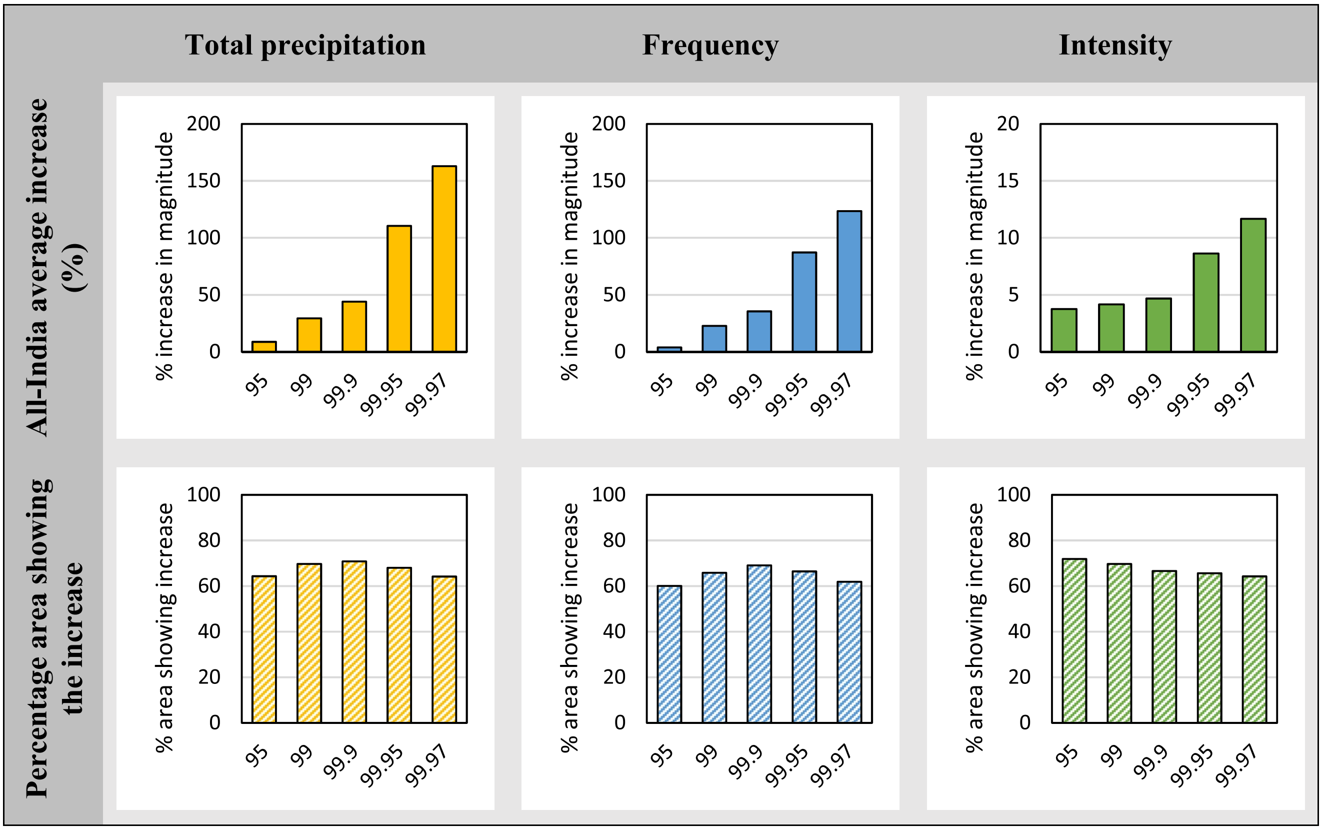

Figure 5. Area-averaged increase (top row) and spatial extent of the increase (bottom row) in total precipitation, frequency, and intensity in the post-1980 period compared to pre-1980 period across Indian mainland for all five percentiles.

the majority of the Indian mainland is experiencing more frequent and more intense rainfall events as compared to its other counterparts in the post-1980 period.

However, this observation of gradually increasing rate of increase in *TP*, *F*, and *I* with the extremeness of the threshold percentile does not hold in the case of spatial extent (percentage of total Indian mainland) of areas showing the increase in *TP*, *F*, and *I* (bottom row of Figure 5). Instead, the area showing the increase in *TP*, *F*, and *I* remains more or less same beyond a certain threshold of extreme. However, approximately two-thirds of the entire Indian mainland (∼66%) exhibits an increase in precipitation extremes, which is quite alarming.

Table 3
Quantitative Estimates of Observed Increases in Total Precipitation, Frequency, and Intensity in Post-1980 Period Compared to Pre-1980 Period Across Indian Mainland

Extreme threshold percentile	Percentage increase in magnitude			Percentage area (spatial extent) showing increase		
	TP	*F*	*I*	*TP*	*F*	*I*
95.00	8.70	3.90	3.75	59.29	55.08	69.88
99.00	29.46	22.85	4.16	65.69	63.86	66.66
99.90	44.00	35.55	4.68	66.79	66.11	64.65
99.95	110.49	87.26	8.63	64.03	63.42	63.66
99.97	162.87	123.54	11.67	60.15	57.83	63.26

Note. TP: Total Precipitation (mm), *F*: Frequency (year^{-1}), and *I*: Intensity (mm/day) above the respective extreme threshold percentile.

4.2.2. HPZ-Wise Analysis

In the previous section, an overall increasing pattern of frequency-dominant precipitation extremes is observed in the majority of parts of India after the year 1980 under a possible impact of the global climatic shift. However, there is a diverse spatial variation in the changing pattern of *TP*, *F*, and *I*. Thus, an HPZ-wise (as identified before) analysis is carried out to investigate how different zones of homogeneous precipitation characteristics respond to these changes. Toward this, the area-averaged values of changes in *TP*, *F*, and *I* for all five extreme thresholds are obtained, which shows that the all-India observation of a frequency-dominated increase in precipitation extremes holds true for all six HPZs individually, as shown in Figure S5a in Supporting Information S1. A further comparative study is done among the HPZs to understand the inter-zonal variation of changes, and the results are presented in Figure 7 in the form of bar plots, which depicts some very interesting features.

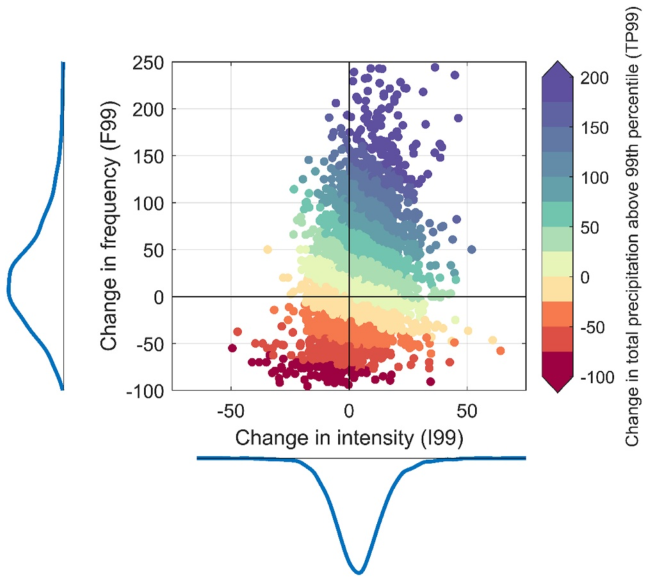

Figure 6. Scatter plot between the observed changes in F99 and I99 for all grid-points across Indian mainland, with a colorbar showing the corresponding changes in TP99.

The pattern of changes in precipitation extremes is completely opposite in high- and low-seasonality zones. In the case of high-seasonality zones (HPZ-1, 2, and 3), the extent of increase in *TP* and *F* gradually becomes higher with the increase in precipitation. Thus, among the low seasonality zones, the highest amount of increase is noticed in the case of HPZ-3 (P_HS_H: Western Ghats), followed by HPZ-2 (P_MS_H), and the least increase in the case of HPZ-1 (P_LS_H: Arid regions over western India). In contrast, for low-seasonality zones (HPZ-4, 5, and 6), the extent of increase in *TP* and *F* reduces with the increase in mean annual precipitation. Thus, the maximum amount of increase is noticed in the case of HPZ-4 (P_LS_L: peninsular India), followed by HPZ-5 (P_MS_L: Eastern part of India) and the minimum increase in the case of HPZ-6 (P_HS_L: North-east India). In general, the HPZ-3 or Western Ghats and the HPZ-4 or Peninsular India, thus in total the southern half of the country exhibits the maximum extent of increase in total precipitation and frequency for all levels of extremeness. In the case of lower extremes (like 95th or 99th percentile), the HPZ-5, that is, eastern India and eastern coast portion also shows a good amount of increase. However, in the case of higher extremes (like 99.95th or 99.97th percentiles), the HPZ-2 shows a considerable amount of increase in *TP* and *F*, in some cases at par with HPZ-3.

Similar observations hold partially true for intensity as well, where the north-east India (HPZ-6), that is, the climatologically high-precipitation zone, is showing the least amount of increase. On the other hand, the climatologically low precipitation zones, such as Peninsular India (HPZ-4) and North-west India (HPZ-1) exhibit maximum amount of increases, particularly for the higher extremes. The extent of increase in intensity across the remaining zones, such as HPZ-2, 3, and 5 remains moderate to low. For further details, readers can refer to Section A3 in Supporting Information S1.

In a nutshell, the southern part of India—including the low-precipitation low-seasonality zone in peninsular India or HPZ-4 and the high-precipitation low-seasonality zone HPZ-3 in western Ghats or HPZ-3, shows a considerable amount of increase in all three characteristics of extreme precipitation—total precipitation, frequency, and intensity. On contrary, the extent of increase is comparatively weaker in northern India, and weakest in north-east India, which otherwise belongs to a climatologically high precipitation zone.

4.3. Future-Projected Changes in Precipitation Extremes: Multi-Model Assessment

4.3.1. All-India Analysis

Average values from all 14 CMIP6-GCM (hereinafter, multi-model ensemble mean) outputs are analyzed to detect the future changes in precipitation extremes in terms of *TP*, *F*, and *I* across the Indian mainland. The results are shown in Figures 8 and 9 as the spatial distribution of ensemble mean changes in precipitation extremes over near-future and far-future period w.r.t. the base period (1981–2010) for SSP245 and SSP585, respectively, considering all five levels of extreme threshold. The individual changes in *TP*, *F*, and *I* for all 14 GCMs are shown in Figures S2–S4 in Supporting Information S1, respectively, over the far-future period for one extreme threshold only (99th percentile), which shows a substantial inter-model variation. However, the multi-model ensemble mean from all 14 models (Figures 8 and 9) shows a more robust estimate of the changes in precipitation extremes, and thus, presents a more homogeneous pattern of changes as compared to the individual models. From these figures, it is noticed that all three attributes of precipitation extremes—total precipitation, frequency and intensity, exhibit an increase over almost entire India in the future, especially in the western coastal regions in South India and north-west parts of India. Also, the increase in all three attributes of extreme precipitation—*TP*, *F* and *I*, becomes more pronounced with the increase in the extremeness of the events, similar to observational analysis.

However, the spatial pattern of future changes in precipitation extremes differs from the observational changes. From the observational analysis of the post-1980 period (w.r.t pre-1980 period), it was noticed that the eastern coast of South India predominantly exhibits an increase in precipitation extremes. However, in the future, the western coast of south India shows a higher extent of increase than the eastern coast. A similar observation was

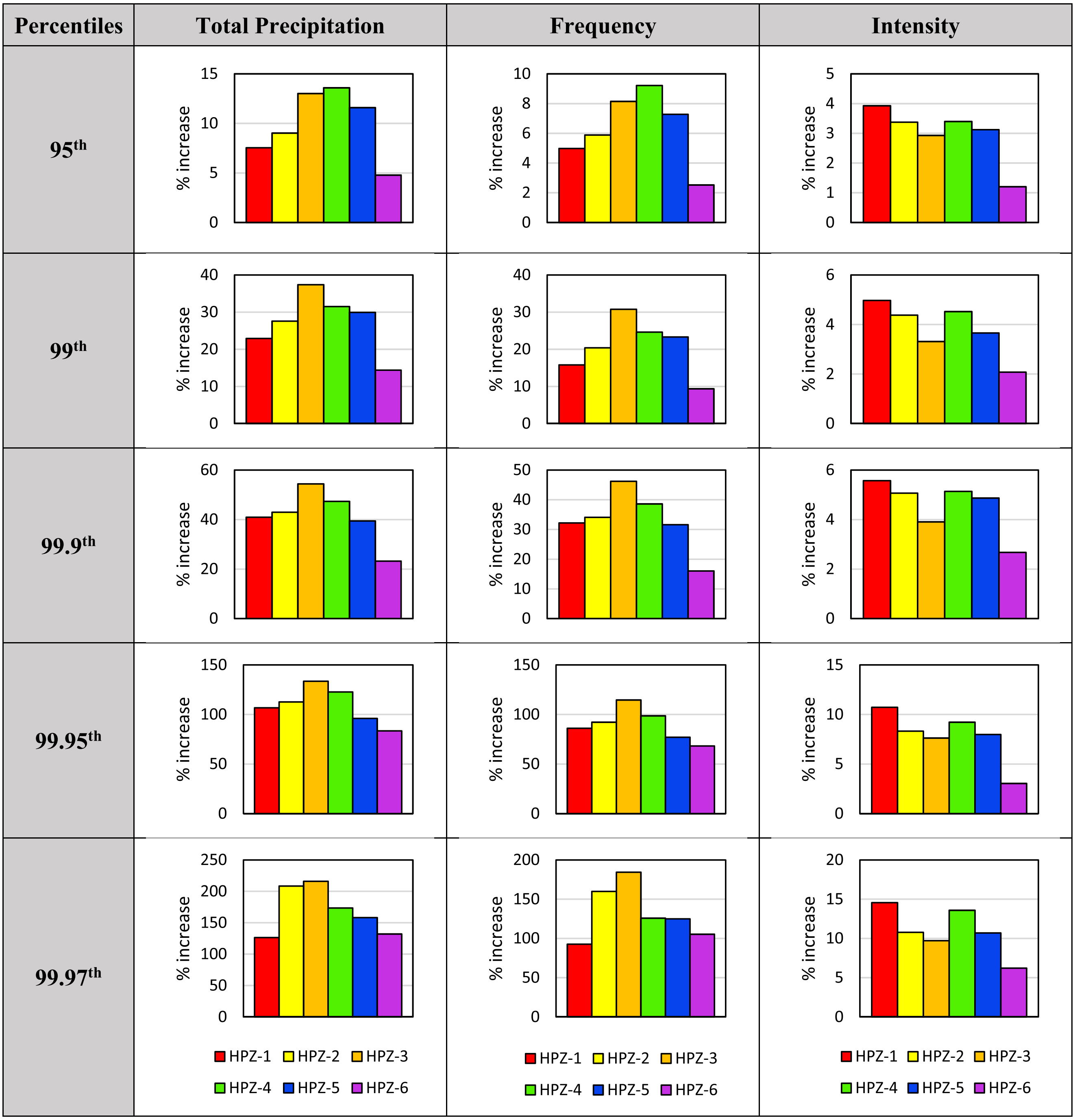

Figure 7. Comparison of the changes in total precipitation, frequency and intensity between six Homogeneous Precipitation Zones (HPZs) for all five extreme thresholds.

also made by an earlier study (Suman & Maity, 2020), where CMIP5-Coordinated Regional Climate Downscaling Experiment (CORDEX) data were analyzed. However, the increase was in general across southern India, irrespective of the eastern/western coast of South India.

In general, the quantitative outcomes of the comparative analysis between near- and far-future periods with respect to the recent past (post-1980 period) are summarized in Table 4 and Figure 10. It is noticed that the multi-model ensemble mean changes in *TP*, *F*, and *I* are substantially higher in the far-future period, as compared to the near-future period, especially under the worst scenario of SSP585. This suggests the continuation of the

10.1029/2021JD035539

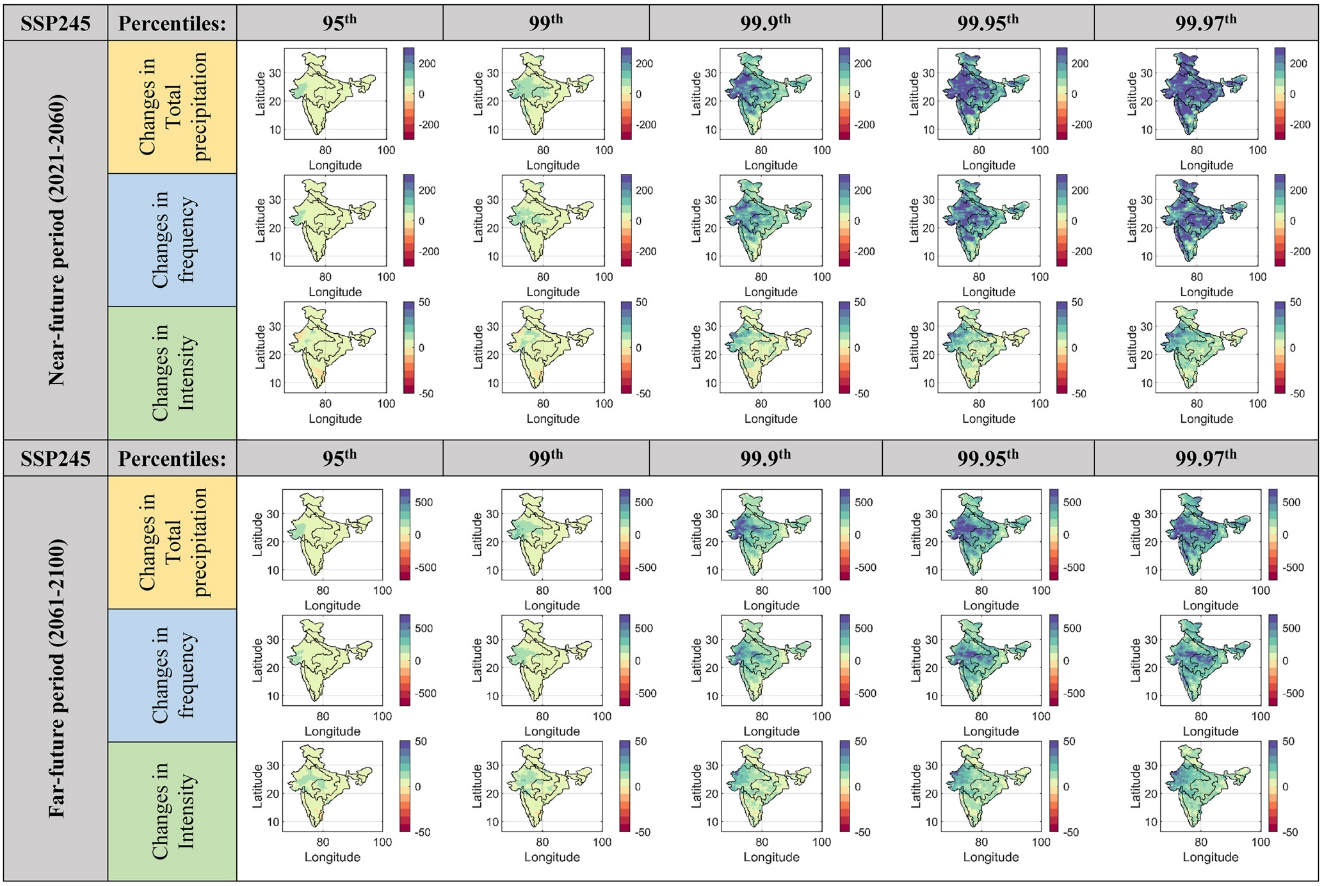

Figure 8. Future-projected ensemble mean changes (in percentage) in total precipitation, frequency and intensity over near-future (top) and far-future (bottom) period as compared to post-1980 reference across Indian mainland following SSP245 for all five thresholds of extreme precipitation.

increasing pattern of precipitation extremes through this century. Also, if we compare the results of SSP245 and SSP585, the increase is more pronounced in the case of SSP585, especially in the far-future period. This observation confirms the role of anthropogenic forcings toward the increase of extreme precipitation in the future.

Similar to the analysis performed in the historical period, a gradual increase is noticed in total precipitation, frequency and intensity above a certain threshold over the future with the increase in the extremeness of the threshold. Therefore, more intense and more frequent precipitation extremes are expected in future across the country. Similar to the observed changes, the changes in total precipitation are noticed to be mostly dominated by changes in frequency in future also. However, as before, the contribution from changes in intensity cannot be denied.

To further investigate the changing pattern of frequency, the annual time series (1951–2100) of the multi-model ensemble mean frequency of the 99th percentile (F99) events is plotted in Figure 11 across the Indian mainland. F99 from individual CMIP6 models and their ensemble mean are obtained for the historical (1951–2014) and future (2015–2100) simulation periods, considering the pre-1980 (1951–1980) period as the reference period. Notably, a steady increasing trend from the historical to future period in frequency is noticed, that becomes more noticeable after the 2050s, that is, in the far-future period. It is further noticed that a mostly comparable or slightly higher frequency under SSP585 than SSP245 in the near-future period, but the difference becomes more apparent toward the end of the century. An approximately average frequency of 1 events per year in the 1950s increases almost threefold by 2100, which is a quite substantial increase in F99 across the Indian mainland under the worst scenario. However, it is also noticed that the inter-model variations increase with the passage of time in this 21st century. This could be attributed to inter-model differences in simulating the surface temperature. Earlier studies have found that models showing the strongest (weakest) increase in frequency, also have the strongest (weakest) surface temperature increase (Myhre et al., 2019).

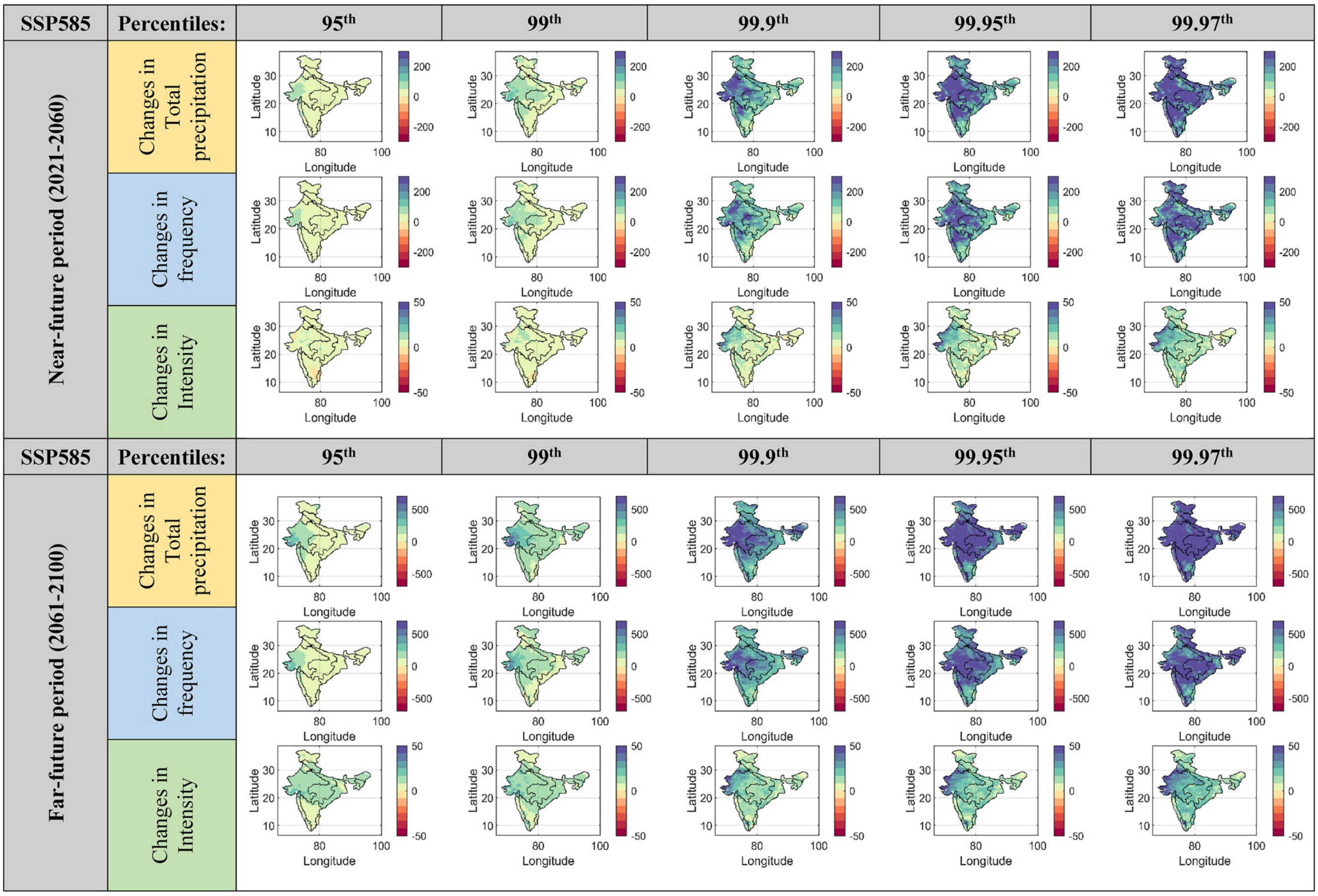

Figure 9. Same as Figure 8, but for SSP585.

The multi-model ensemble mean changes in precipitation extremes (*TP*, *F*, and *I*) in the far-future period are shown in Figure 12 (left panel). For comparison, the observed changes in the post-1980 period are also plotted in the same figure. It is noticed that the observed rate of increase in precipitation extremes is going to enhance further in the far-future period, especially under SSP585 scenario. Moreover, the right panel of Figure 12 shows the likely changes in the pdfs of *TP*, *F*, and *I* in the future period for 99th percentile only. From this figure, it can be interpreted how the pdfs of *TP*, *F*, and *I* in the base-period 1981–2010 (blue) shift toward the higher values in the near-future (solid line) and far-future (dotted line) period. The shift is more prominent for frequency than intensity, and in the case of the far-future period following SSP585. It is further noticed that the pdfs in the

Table 4
Quantitative Estimates of Multi-Model Future Changes in Total Precipitation, Frequency, and Intensity as Compared to Post-1980 Period Across Indian Mainland

	SSP245						SSP585					
	Near-future period (2021–2060)			Far-future period (2061–2100)			Near-future period (2021–2060)			Far-future period (2061–2100)		
Extreme threshold percentile	TP	F	I	TP	F	I	TP	F	I	TP	F	I
95.00	23.82	19.55	3.42	54.99	46.50	5.46	31.70	26.72	3.84	111.38	89.87	10.92
99.00	43.09	36.35	3.86	89.95	76.38	6.29	53.91	46.05	4.23	193.93	156.41	12.01
99.90	138.18	114.81	8.11	249.54	206.05	10.03	156.83	130.89	8.52	481.87	407.71	15.83
99.95	204.42	166.36	11.18	351.73	286.79	12.74	229.90	188.46	11.64	633.90	540.79	18.84
99.97	246.19	196.06	14.44	404.98	323.26	15.70	271.99	217.80	14.74	679.57	601.88	21.99

Note. TP: Total Precipitation (mm), *F*: Frequency (year^{-1}), and *I*: Intensity (mm/day) above the respective extreme threshold percentile.

10.1029/2021JD035539

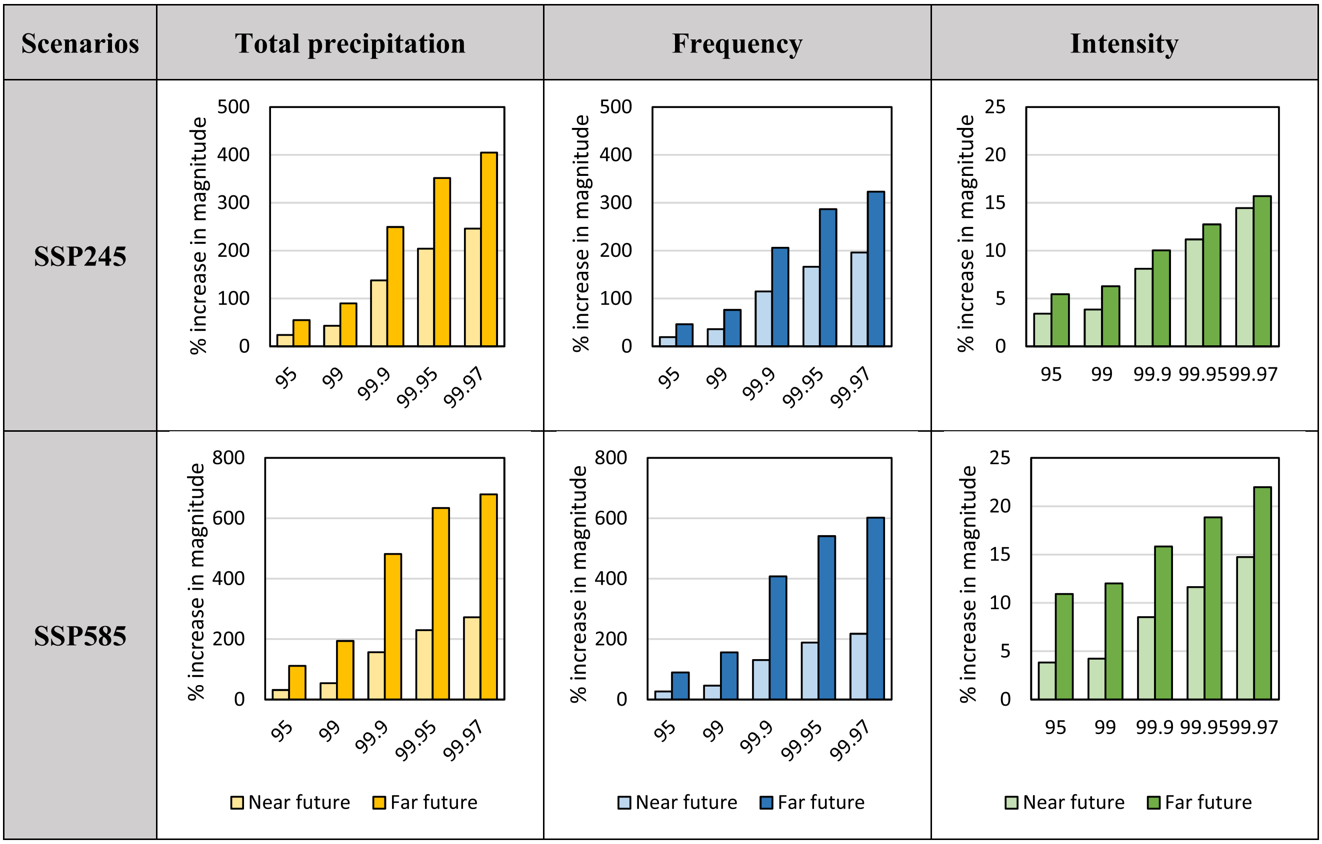

Figure 10. Multi-model ensemble average changes in total precipitation, frequency, and intensity over near-future and far-future period in India, following SSP245 (top) and SSP585 (bottom).

near-future period are more or less comparable under both the scenarios, but differ noticeably in the far-future period. Overall, a substantial shift in the underlying distribution toward higher values of precipitation extremes is expected in the future, resulting in an increase in precipitation extremes across the Indian mainland.

4.3.2. HPZ-Wise Analysis

Similar to the analysis performed in the historical period, the HPZ-wise analysis is also performed here to investigate how these different precipitation zones will experience future changes in precipitation extremes. The results are summarized in Figure 13 (for inter-HPZ comparison) and Figure S5 in Supporting Information S1 (panel b and panel c, for comparison among *TP*, *F* and *I*) for the far-future period only, considering both SSP245 and SSP585. It is found that HPZs respond differently to different levels of extreme events. In the case of very rare events (like 99.95th or 99.97th percentile thresholds), the maximum extent of increase in total precipitation and frequency is noticed for climatologically high-precipitation zones such as HPZ-3 and HPZ-6, that is, the Western Ghats regions and north-east India. However, in the case of intensity, the climatologically low precipitation zones, such as HPZ-1 (north-west India) and HPZ-4 (peninsular India) exhibit the highest extent of increase. On the other hand, in the case of lower extreme events (like 95th percentile), the climatologically arid or semi-arid regions like HPZ-1 is showing maximum extent of increase in precipitation extremes (*TP*, *F* and *I*). However, in general, wet places like western Ghats and north-east India are showing a consistently high level of increase in frequency, and comparatively dry regions like north-west and peninsular India exhibit a high level of increase in intensity in extreme precipitation toward the end of this century.

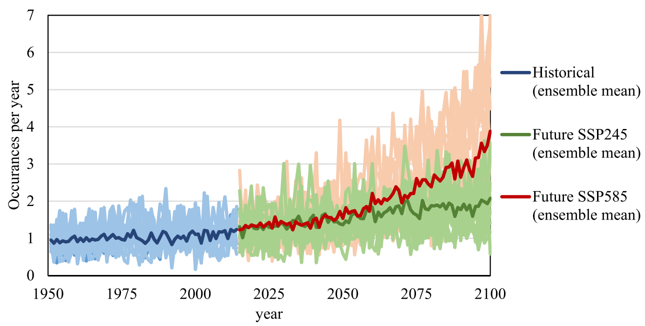

Figure 11. Annual time series plot of all-India average frequency of 99th percentile of precipitation simulated by 14 CMIP6 models for historical (1951–2014) and future (2015–2100) simulation periods. The light color shows the inter-model variations, and the dark color indicates the multi-model ensemble mean.

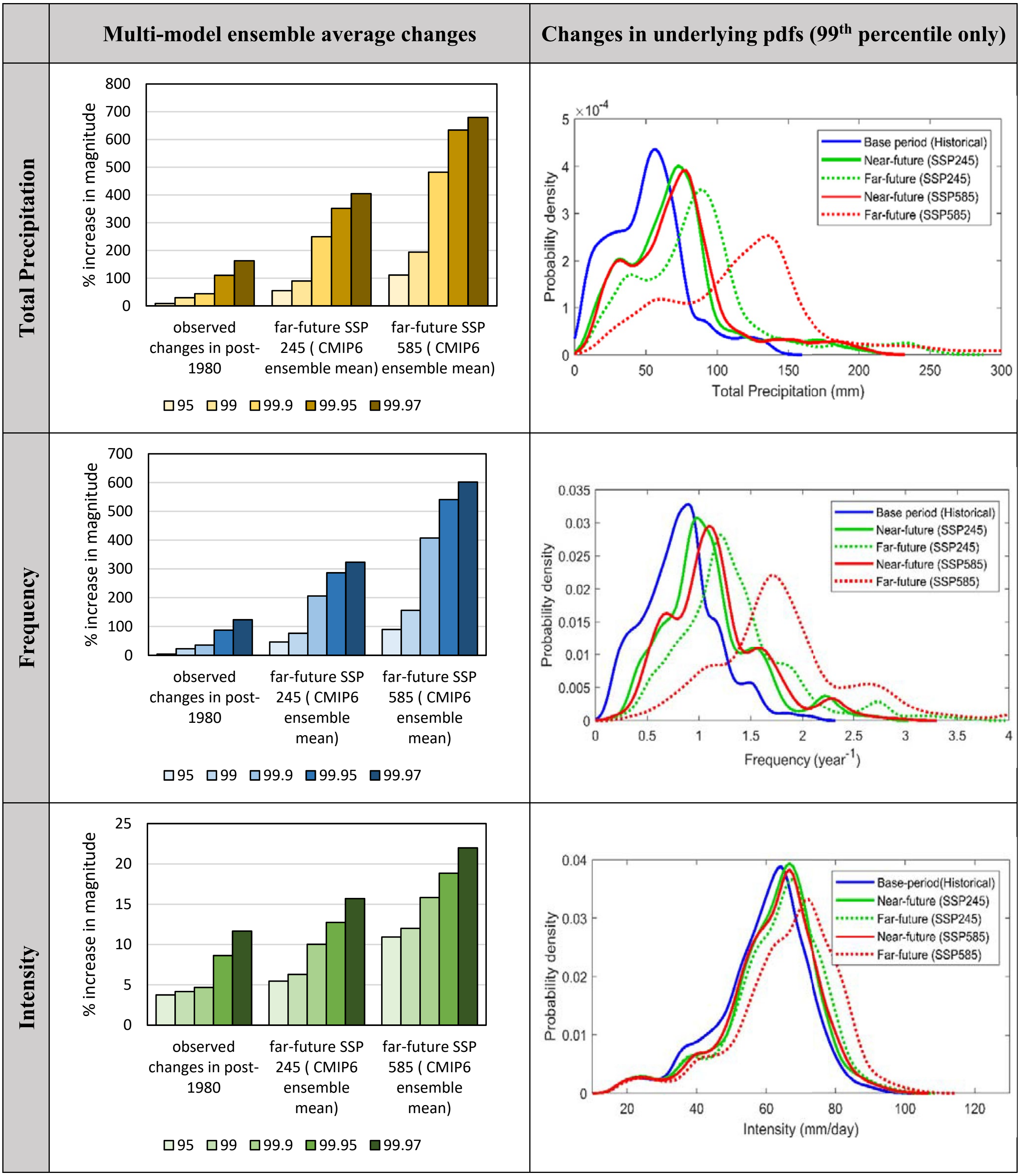

Figure 12. Multi-model ensemble mean changes of *TP*, *F*, and *I* over the far-future period following SSP245 and SSP585 (left panel) and corresponding changes in the underlying pdfs (right panel) for one extreme threshold, i.e., 99th percentile.

In a nutshell, the characteristics of extreme precipitation are projected to enhance across India in future. Such increasing pattern is observed since the second half of the last century and is expected to continue in the present century too, with an almost similar or even higher rate. We specifically highlight the dominance of frequency

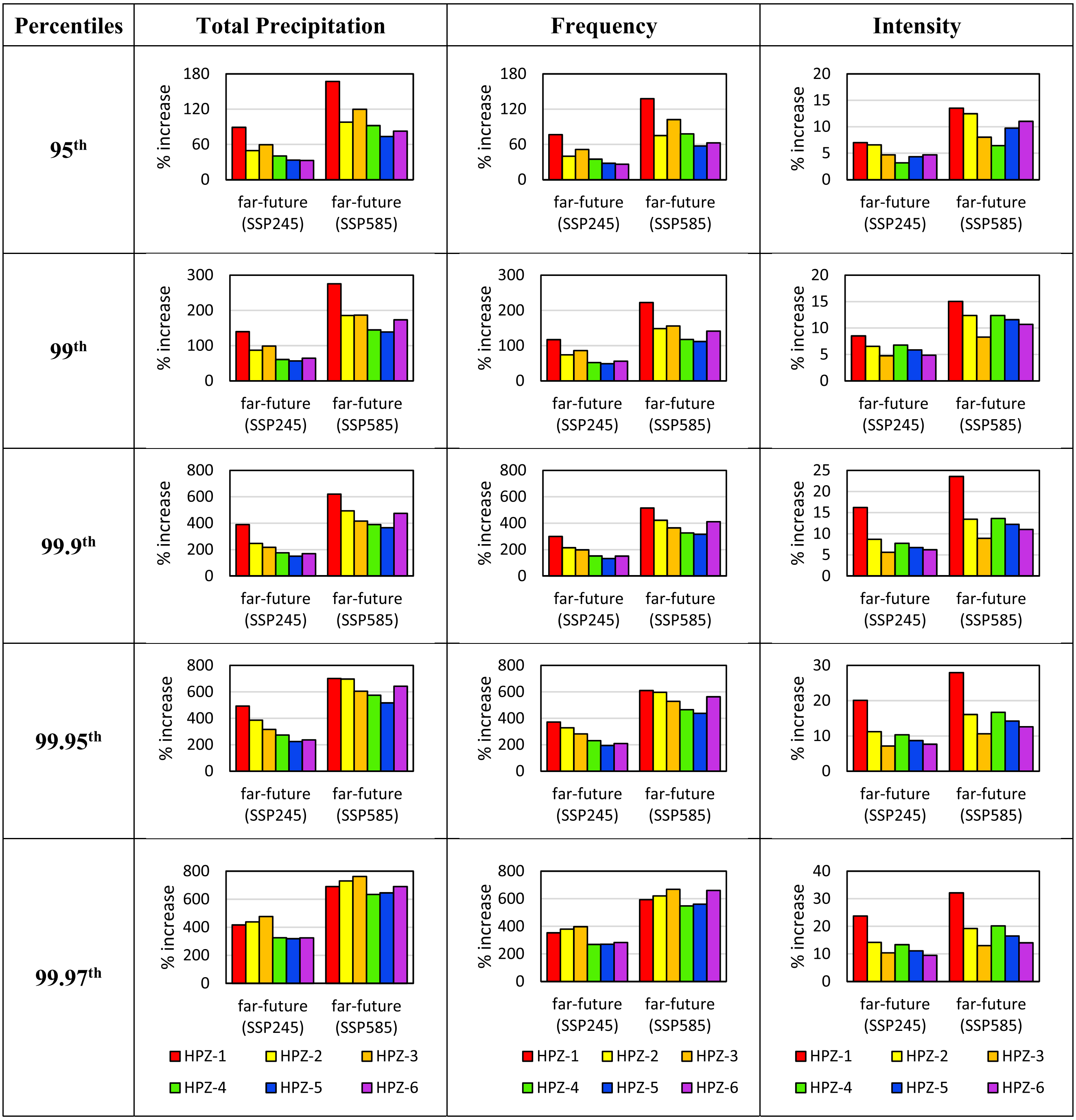

Figure 13. Homogeneous Precipitation Zone (HPZ)-wise comparison of the changes in total precipitation, frequency and intensity in far future period for all five extreme thresholds considered in this study.

changes toward the changes in total extreme precipitation. However, intensity is also projected to increase in most part of India, especially in the climatologically low precipitation zones such as HPZ-1 and HPZ-4. On the other hand, high-precipitation zones such as, HPZ-3 (Western Ghats) and −6 (north-east India) show the maximum increase in frequency over the future. Regardless of inter-model variations, an overall frequency-dominated increase in extreme precipitation is confirmed by all 14 CMIP6-GCMs considered in this study. However, it is worthwhile to note here that these reported results are subjected to various sources of uncertainty. For example, despite using 14 state-of-the-art CMIP6-GCMs, the number and choice of the models and consideration of a single realization per model may not be sufficient enough to capture the full range of uncertainty from the perspective of global climate sensitivity and regional response to global warming (Milinski et al., 2020; Taylor et al., 2012). Therefore, although the multi-model averages are determined, the final results could be sensitive to the number of models and the realization considered—which is a definite limitation of this study. Furthermore, the direct use of the raw GCM simulations can be considered as another source of uncertainty. In general, the GCMs are found to produce precipitation output having significant amount of systematic bias due to their coarse resolution or model parameterizations. Though here we are using a relative metric to quantify the future changes, the potential effect of bias in the results are inevitable. Nonetheless, the overall findings of this study cannot be denied—such level of increases in precipitation extremes must be considered in the climate change adaptation and mitigation strategies to get prepared for the upcoming future.

4.4. Possible Physical Reasoning Behind Increased Precipitation Extremes Across India

In general, the possible physical reasoning behind this increased frequency and intensity of precipitation extremes is difficult to ascertain, except the general consequence of changing climate and increased anthropogenic activities. Stated this, we like to mention that a recent study by Suman and Maity (2020), utilizing future projections from multiple CMIP5-CORDEX simulations, may throw some light on this. Suman and Maity (2020) considered the entire South Asia domain including the Indian Ocean region to understand the plausible dynamics behind the increasing precipitation extremes over India. Though CMIP5 was used, the multi-model analysis revealed a non-uniform spatial pattern of increasing air temperature and vertically integrated precipitation water over the entire domain of south Asia. In particular, a significant increase in air temperature was projected over the Tibetan Plateau and the Himalayas—a hopping 5°C increase toward the end of the century under the worst climate change scenario. On the other hand, the precipitable water was also shown to increase significantly over the Indian Ocean region. These two factors, coupled with potentially enhanced Indian Ocean Dipole (Cai et al., 2013) may create a favorable physical condition for Indian Summer Monsoon (ISM). All these factors may eventually result in increased extremes in various parts of the country. In addition to that, overall increased air temperature throughout India, particularly in the north-west portion or HPZ-1 (Mishra et al., 2020) may augment the possibility of an increased moisture-holding capacity of the atmospheric column following the Clausius-Clapeyron relationship (Trenberth, 2011), resulting in more extreme precipitation events over north-west India. Moreover, a recent study by Singh et al. (2022) evidently identified the increased surface pressure over the Tibetan plateau as a prime factor behind such increased precipitation over north-west India.

Further analysis by Suman and Maity (2020) on moisture flux deviation during the monsoon months reveals an intensification of eastward moisture flux over the Indian Ocean and Arabian sea region, resulting in the entry of more moisture-laden wind over south India through the western coast—causing an overall enhancement of precipitation extremes over the southern part of the country. However, due to the existence of the Western Ghats mountain range along the western coast of India, more frequent extreme precipitation events may occur on the windward side (HPZ-3) of the mountain range.

This perhaps explains the reason behind the more projected increase in extreme precipitation over the western coast compared to the eastern coast in future as found in our analysis. However, more insightful analysis involving various variables, such as air temperature, precipitable water, moisture flux and convergence, is indeed required to explain the zone-specific projections of precipitation extremes. So far the physics behind the simulation are concerned, we solely depend on the schemes adopted by different climate models to simulate these afore-said variables. However, these schemes may not be perfect always and hence as a standard practice, we utilize simulation from multiple models while drawing the conclusions. To understand further on the reasoning, an analysis through RCMs forced by the outputs from the GCMs would be adopted. However, this would lead to another direction toward future scope of the study, and not within the scope of the current study.

5. Conclusions

In this study, the observed historical and expected future changes in different characteristics of precipitation extremes (total precipitation, frequency, and intensity) are assessed across the Indian mainland for five different levels of extreme precipitation (95th, 99th, 99.9th, 99.95th, and 99.97th percentiles). Multi-model ensemble mean from 14 state-of-the-art GCMs from CMIP6 are utilized for projections of precipitation extremes over the near-future (2021–2060) and far-future period (2061–2100). The specific conclusions from the study are as follows:

- The change in total precipitation above a certain extreme threshold is a function of changes in its intensity and frequency-both. However, the major contribution comes from the changes in frequency. However, the effect of intensity changes cannot be denied, of course. Such frequency-dominated increase in precipitation extremes is observed in most part of the Indian mainland after the year 1980 and is expected to continue at a similar or even faster rate in the future.
- A strong gradual strengthening of frequency and intensity increase is observed in the historical, as well as future period, leading to an overall increase in total extreme precipitation with the rareness of the precipitation extremes.
- The future changes in precipitation extremes are mostly comparable in the near-future period under SSP245 and SSP585. However, in the far-future period, SSP585 surpasses SSP245 substantially, indicating a possible impact of anthropogenic activities on such an increase in precipitation extremes.
- The HPZ-wise analysis over the historical period reveals that the maximum amount of increase in precipitation extremes is observed in the southern half of the country (HPZ-3 and HPZ-4), whereas the climatologically high precipitation zone HPZ-6 (north-east India) shows the minimum increase.
- However, in the future, the high-precipitation zones such as Western Ghats (HPZ-3) and north-east India (HPZ-6) show the maximum amount of increase in frequency, especially in the case of higher extreme events. For lower extremes, the low-precipitation region (HPZ-1) shows the maximum amount of increase in frequency. Peninsular India (HPZ-4), another low-precipitation zone, shows the highest level of increase in the intensity of precipitation extremes, especially for the higher extreme events.

Finally, this increasing pattern of extreme precipitation is expected to impact the society by increasing the number of its occurrences and/or its intensity. Such substantial increases in frequency and intensity must be considered in the revised planning, designing, and future risk assessment of any high-risk water resources infrastructure.

Data Availability Statement

The daily gridded observed rainfall data set for entire Indian mainland is obtained from of the India Meteorological Department (IMD), as mentioned in the in-text data citation reference Pai et al. (2014), and also can be accessed online via https://www.imdpune.gov.in/Clim_Pred_LRF_New/Grided_Data_Download.html. The simulated future daily precipitation datasets (2021–2100) are obtained from 14 state-of-the-art GCMs from the Earth system Grid Federation Archive, that is, https://esgf-node.llnl.gov/search/cmip6/. All the figures in this manuscript are prepared using either MATLAB software (version R2021a, URL: https://in.mathworks.com) or Microsoft EXCEL 2016.

Acknowledgments
This work is partially supported by the Ministry of Earth Science, Government of India through a sponsored project. The authors further acknowledge the National Supercomputing Mission (NSM) for providing computing resources of "PARAM Shakti" at IIT Kharagpur, which is implemented by C-DAC and supported by the Ministry of Electronics and Information Technology (MeitY) and Department of Science and Technology (DST), Government of India. Finally, the authors thank the editors and two anonymous reviewers whose constructive comments immensely improved the manuscript.

References

Abdelmoaty, H. M., Papalexiou, S. M., Rajulapati, C. R., & AghaKouchak, A. (2021). Biases beyond the mean in CMIP6 extreme precipitation: A global investigation. *Earth's Future*, *9*(10), 1–17. https://doi.org/10.1029/2021EF002196

Alexander, L. V., Zhang, X., Peterson, T. C., Caesar, J., Gleason, B., Klein Tank, A. M. G., et al. (2006). Global observed changes in daily climate extremes of temperature and precipitation. *Journal of Geophysical Research*, *111*(5), 1–22. https://doi.org/10.1029/2005JD006290

Allan, R. P., Liu, C., Zahn, M., Lavers, D. A., Koukouvagias, E., & Bodas-Salcedo, A. (2014). Physically consistent responses of the global atmospheric hydrological cycle in models and observations. *Surveys in Geophysics*, *35*(3), 533–552. https://doi.org/10.1007/s10712-012-9213-z

Allen, M. R., & Ingram, W. J. (2002). Constraints on future changes in climate and the hydrologic cycle. *Nature*, *419*, 228–232. https://doi.org/10.1038/nature01092

Ashfaq, M., Rastogi, D., Mei, R., Touma, D., & Ruby Leung, L. (2017). Sources of errors in the simulation of south Asian summer monsoon in the CMIP5 GCMs. *Climate Dynamics*, *49*(1–2), 193–223. https://doi.org/10.1007/s00382-016-3337-7

Barbero, R., Fowler, H. J., Lenderink, G., & Blenkinsop, S. (2017). Is the intensification of precipitation extremes with global warming better detected at hourly than daily resolutions? *Geophysical Research Letters*, *44*(2), 974–983. https://doi.org/10.1002/2016GL071917

Berg, P., Moseley, C., & Haerter, J. O. (2013). Strong increase in convective precipitation in response to higher temperatures. *Nature Geoscience*, *6*(3), 181–185. https://doi.org/10.1038/ngeo1731

Bhatla, R., Ghosh, S., Verma, S., Mall, R. K., & Gharde, G. R. (2019). Variability of monsoon over homogeneous regions of India using regional climate model and impact on crop production. *Agricultural Research*, *8*(3), 331–346. https://doi.org/10.1007/s40003-018-0368-9

Cai, W., Zheng, X. T., Weller, E., Collins, M., Cowan, T., Lengaigne, M., et al. (2013). Projected response of the Indian Ocean dipole to greenhouse warming. *Nature Geoscience*, *6*(12), 999–1007. https://doi.org/10.1038/ngeo2009

Chen, C. A., Hsu, H. H., & Liang, H. C. (2021). Evaluation and comparison of CMIP6 and CMIP5 model performance in simulating the seasonal extreme precipitation in the Western North Pacific and East Asia. *Weather and Climate Extremes*, *31*, 100303. https://doi.org/10.1016/j.wace.2021.100303

Chen, H., He, D., & Zhu, Z. (2019). The internal multidecadal variability of SST in the Pacific and its impact on air temperature and rainfall over land in the Northern Hemisphere. *Atmosphere*, *10*(3), 153. https://doi.org/10.3390/atmos10030153

Christensen, J. H., Boberg, F., Christensen, O. B., & Lucas-Picher, P. (2008). On the need for bias correction of regional climate change projections of temperature and precipitation. *Geophysical Research Letters*, *35*(20), L20709. https://doi.org/10.1029/2008GL035694

Dai, T., Dong, W., Guo, Y., Hong, T., Ji, D., Yang, S., et al. (2018). Understanding the abrupt climate change in the mid-1970s from a phase-space transform perspective. *Journal of Applied Meteorology and Climatology*, *57*(11), 2551–2560. https://doi.org/10.1175/JAMC-D-17-0345.1

Dash, S., & Maity, R. (2019). Temporal evolution of precipitation-based climate change indices across India: Contrast between pre- and post-1975 features. *Theoretical and Applied Climatology*, *138*(3–4), 1667–1678. https://doi.org/10.1007/s00704-019-02923-8

Dash, S. K., Shekhar, M. S., Singh, G. P., & Vernekar, A. D. (2002). Relationship between surface fields over Indian Ocean and monsoon rainfall over homogeneous zones of India. *Mausam*, *53*(2), 133–144. https://doi.org/10.54302/mausam.v53i2.1629

Deng, Y., Jiang, W., He, B., Chen, Z., & Jia, K. (2018). Change in intensity and frequency of extreme precipitation and its possible teleconnection with large-scale climate index over the China from 1960 to 2015. *Journal of Geophysical Research: Atmospheres*, *123*(4), 2068–2081. https://doi.org/10.1002/2017JD027078

De Souza, K., Kituyi, E., Harvey, B., Leone, M., Murali, K. S., & Ford, J. D. (2015). Vulnerability to climate change in three hot spots in Africa and Asia: Key issues for policy-relevant adaptation and resilience-building research. *Regional Environmental Change*, *15*(5), 747–753. https://doi.org/10.1007/s10113-015-0755-8

Di Luca, A., Pitman, A. J., & de Elía, R. (2020). Decomposing temperature extremes errors in CMIP5 and CMIP6 models. *Geophysical Research Letters*, *47*(14), 1–10. https://doi.org/10.1029/2020GL088031

Ehret, U., Zehe, E., Wulfmeyer, V., Warrach-Sagi, K., & Liebert, J. (2012). HESS Opinions "should we apply bias correction to global and regional climate model data?". *Hydrology and Earth System Sciences*, *16*(9), 3391–3404. https://doi.org/10.5194/hess-16-3391-2012

Eyring, V., Bony, S., Meehl, G. A., Senior, C. A., Stevens, B., Stouffer, R. J., et al. (2016). Overview of the coupled model Intercomparison Project phase 6 (CMIP6) experimental design and organization. *Geoscience Model Development*, *9*(5), 1937–1958. https://doi.org/10.5194/gmd-9-1937-2016

Fischer, E. M., & Knutti, R. (2016). Observed heavy precipitation increase confirms theory and early models. *Nature Climate Change*, *6*(11), 986–991. https://doi.org/10.1038/nclimate3110

Ghosh, S., Das, D., Kao, S. C., & Ganguly, A. R. (2012). Lack of uniform trends but increasing spatial variability in observed Indian rainfall extremes. *Nature Climate Change*, *2*(2), 86–91. https://doi.org/10.1038/nclimate1327

Gidden, M. J., Riahi, K., Smith, S. J., Fujimori, S., Luderer, G., Kriegler, E., et al. (2019). Global emissions pathways under different socioeconomic scenarios for use in CMIP6: A dataset of harmonized emissions trajectories through the end of the century. *Geoscientific Model Development*, *12*(4), 1443–1475. https://doi.org/10.5194/gmd-12-1443-2019

Giorgi, F., Coppola, E., & Raffaele, F. (2014). A consistent picture of the hydroclimatic response to global warming from multiple indices: Models and observations. *Journal of Geophysical Research*, *119*(20), 11695–11708. https://doi.org/10.1002/2014JD022238

Giorgi, F., Im, E.-S., Coppola, E., Diffenbaugh, N. S., Gao, X. J., Marotti, L., & Shi, Y. (2011). Higher hydroclimatic intensity with global warming. *Journal of Climate*, *24*(20), 5309–5324. https://doi.org/10.1175/2011JCLI3979.1

Guhathakurta, P., Sreejith, O. P., & Menon, P. A. (2011). Impact of climate change on extreme rainfall events and flood risk in India. *Journal of Earth System Science*, *120*(3), 359–373. https://doi.org/10.1007/s12040-011-0082-5

Hennessy, K. J., Gregory, J. M., & Mitchell, J. F. B. (1997). Changes in daily precipitation under enhanced greenhouse conditions. *Climate Dynamics*, *13*(9), 667–680. https://doi.org/10.1007/s003820050189

Jacob, D., & Hagemann, S. (2007). Intensification of the hydrological cycle – an important signal of climate change (pp. 170–173).

Kao, S. C., & Ganguly, A. R. (2011). Intensity, duration, and frequency of precipitation extremes under 21st-century warming scenarios. *Journal of Geophysical Research*, *116*(16), 1–14. https://doi.org/10.1029/2010JD015529

Kharin, V. V., Zwiers, F. W., Zhang, X., & Wehner, M. (2013). Changes in temperature and precipitation extremes in the CMIP5 ensemble. *Climatic Change*, *119*(2), 345–357. https://doi.org/10.1007/s10584-013-0705-8

Knutti, R., Furrer, R., Tebaldi, C., Cermak, J., & Meehl, G. A. (2010). Challenges in combining projections from multiple climate models. *Journal of Climate*, *23*(10), 2739–2758. https://doi.org/10.1175/2009JCLI3361.1

Kothawale, D. R., & Rajeevan, M. (2017). Monthly, seasonal and annual rainfall time series for All-India, homogeneous regions and Meteorological Subdivisions : 1871–2016. *Indian Institute of Tropical Meteorology (IITM) Earth System Science Organization, Ministry of Earth Sciences*, *02*, 1–164.

Kunstmann, H., Schneider, K., Forkel, R., & Knoche, R. (2004). Impact analysis of climate change for an Alpine catchment using high resolution dynamic downscaling of ECHAM4 time slices. *Hydrology and Earth System Sciences*, *8*(6), 1031–1045. https://doi.org/10.5194/hess-8-1031-2004

Leander, R., & Buishand, T. A. (2007). Resampling of regional climate model output for the simulation of extreme river flows. *Journal of Hydrology*, *332*(3–4), 487–496. https://doi.org/10.1016/j.jhydrol.2006.08.006

Leander, R., Buishand, T. A., van den Hurk, B. J. J. M., & de Wit, M. J. M. (2008). Estimated changes in flood quantiles of the river Meuse from resampling of regional climate model output. *Journal of Hydrology*, *351*(3–4), 331–343. https://doi.org/10.1016/j.jhydrol.2007.12.020

Lenderink, G., Buishand, A., & Van Deursen, W. (2007). Estimates of future discharges of the river Rhine using two scenario methodologies: Direct versus delta approach. *Hydrology and Earth System Sciences*, *11*(3), 1145–1159. https://doi.org/10.5194/hess-11-1145-2007

Li, J., Huo, R., Chen, H., Zhao, Y., & Zhao, T. (2021). Comparative assessment and future prediction using CMIP6 and CMIP5 for annual precipitation and extreme precipitation simulation. *Frontiers of Earth Science*, *9*, 1–20. https://doi.org/10.3389/feart.2021.687976

Lu, E., Zeng, Y., Luo, Y., Ding, Y., Zhao, W., Liu, S., et al. (2014). Changes of summer precipitation in China: The dominance of frequency and intensity and linkage with changes in moisture and air temperature. *Journal of Geophysical Research: Atmospheres*, *119*(22), 12575–12587. https://doi.org/10.1038/175238c0

Madakumbura, G. D., Kim, H., Utsumi, N., Shiogama, H., Fischer, E. M., Seland, Ø., et al. (2019). Event-to-event intensification of the hydrologic cycle from 1.5°C to a 2°C warmer world. *Scientific Reports*, *9*, 1–7. https://doi.org/10.1038/s41598-019-39936-2

Maity, R., Suman, M., Laux, P., & Kunstmann, H. (2019). Bias correction of zero-inflated RCM precipitation fields: A copula-based scheme for both mean and extreme conditions. *Journal of Hydrometeorology*, *20*(4), 595–611. https://doi.org/10.1175/JHM-D-18-0126.1

Mao, G., Vogl, S., Laux, P., Wagner, S., & Kunstmann, H. (2015). Stochastic bias correction of dynamically downscaled precipitation fields for Germany through copula-based integration of gridded observation data. *Hydrology and Earth System Sciences*, *19*(4), 1787–1806. https://doi.org/10.5194/hess-19-1787-2015

Maraun, D. (2016). Bias correcting climate change simulations—A critical review. *Current Climate Change Reports*, *2*(4), 211–220. https://doi.org/10.1007/s40641-016-0050-x

Milinski, S., Maher, N., & Olonscheck, D. (2020). How large does a large ensemble need to be? *Earth System Dynamics*, *11*(4), 885–901. https://doi.org/10.5194/esd-11-885-2020

Mishra, V. (2020). Long-term (1870–2018) drought reconstruction in context of surface water security in India. *Journal of Hydrology*, *580*, 124228. https://doi.org/10.1016/j.jhydrol.2019.124228

Mishra, V., Bhatia, U., & Tiwari, A. D. (2020). Bias-corrected climate projections for South Asia from Coupled Model Intercomparison Project-6. *Scientific Data*, *7*(1), 1–10. https://doi.org/10.1038/s41597-020-00681-1

Mishra, V., Kumar, D., Ganguly, A. R., Sanjay, J., Mujumdar, M., Krishnan, R., & Shah, R. D. (2014). Reliability of regional and global climate models to simulate precipitation extremes over India. *Journal of Geophysical Research: Atmospheres*, *119*(15), 3672–3685. https://doi.org/10.1002/2014JD021636

Mishra, V., Wallace, J. M., & Lettenmaier, D. P. (2012). Relationship between hourly extreme precipitation and local air temperature in the United States. *Geophysical Research Letters*, *39*(16), 1–7. https://doi.org/10.1029/2012GL052790

Mukherjee, S., Aadhar, S., Stone, D., & Mishra, V. (2018). Increase in extreme precipitation events under anthropogenic warming in India. *Weather and Climate Extremes*, *20*, 45–53. https://doi.org/10.1016/j.wace.2018.03.005

Myhre, G., Alterskjær, K., Stjern, C. W., Hodnebrog, Ø., Marelle, L., Samset, B. H., et al. (2019). Frequency of extreme precipitation increases extensively with event rareness under global warming. *Scientific Reports*, *9*(1), 1–10. https://doi.org/10.1038/s41598-019-52277-4

O'Gorman, P. A. (2015). Precipitation extremes under climate change. *Current Climate Change Reports*, *1*(2), 49–59. https://doi.org/10.1007/s40641-015-0009-3

O'Gorman, P. A., Allan, R. P., Byrne, M. P., & Previdi, M. (2012). Energetic constraints on precipitation under climate change. *Surveys in Geophysics*, *33*(3–4), 585–608. https://doi.org/10.1007/s10712-011-9159-6

Ott, I., Duethmann, D., Liebert, J., Berg, P., Feldmann, H., Ihringer, J., et al. (2013). High-resolution climate change impact analysis on medium-sized river catchments in Germany: An ensemble assessment. *Journal of Hydrometeorology*, *14*(4), 1175–1193. https://doi.org/10.1175/JHM-D-12-091.1

Pai, D. S., Sridhar, L., Rajeevan, M., Sreejith, O. P., Satbhai, N. S., & Mukhopadhyay, B. (2014). Development of a new high spatial resolution ($0.25° \times 0.25°$) long period (1901–2010) daily gridded rainfall data set over India and its comparison with existing data sets over the region [Dataset]. Mausam, *65*(1), 1–18. https://doi.org/10.54302/mausam.v65i1.851

Pall, P., Aina, T., Stone, D. A., Stott, P. A., Nozawa, T., Hilberts, A. G. J., et al. (2011). Anthropogenic greenhouse gas contribution to flood risk in England and Wales in autumn 2000. *Nature*, *470*(7334), 382–385. https://doi.org/10.1038/nature09762

Papalexiou, S. M., & Montanari, A. (2019). Global and regional increase of precipitation extremes under global warming. *Water Resources Research*, *55*(6), 1–14. https://doi.org/10.1029/2018WR024067

Parthasarathy, B., Kumar, K. R., & Munot, A. (1996). Homogeneous regional summer monsoon rainfall over India: Interannual variability and teleconnections. *IITM, Pune, Research R*. Retrieved from http://www.tropmet.res.in/~lip/Publication/RR-pdf/RR-70.pdf

Pendergrass, A. G., & Hartmann, D. L. (2014). The atmospheric energy constraint on global-mean precipitation change. *Journal of Climate*, *27*(2), 757–768. https://doi.org/10.1175/JCLI-D-13-00163.1

Piani, C., Haerter, J. O., & Coppola, E. (2010). Statistical bias correction for daily precipitation in regional climate models over Europe. *Theoretical and Applied Climatology*, *99*(1–2), 187–192. https://doi.org/10.1007/s00704-009-0134-9

Pierce, D. W., Cayan, D. R., Maurer, E. P., Abatzoglou, J. T., & Hegewisch, K. C. (2015). Improved bias correction techniques for hydrological simulations of climate change. *Journal of Hydrometeorology*, *16*(6), 2421–2442. https://doi.org/10.1175/JHM-D-14-0236.1

Rajeevan, M., Bhate, J., & Jaswal, A. K. (2008). Analysis of variability and trends of extreme rainfall events over India using 104 years of gridded daily rainfall data. *Geophysical Research Letters*, *35*(18), 1–6. https://doi.org/10.1029/2008GL035143

Rajendran, K., Sajani, S., Jayasankar, C. B., & Kitoh, A. (2013). How dependent is climate change projection of Indian summer monsoon rainfall and extreme events on model resolution? *Current Science*, *104*(10), 1409–1418.

Rajulapati, C. R., Papalexiou, S. M., Clark, M. P., & Pomeroy, J. W. (2021). The perils of regridding: Examples using a global precipitation dataset. *Journal of Applied Meteorology and Climatology*, *11*, 1561–1573. https://doi.org/10.1175/jamc-d-20-0259.1

Reid, P. C., Hari, R. E., Beaugrand, G., Livingstone, D. M., Marty, C., Straile, D., et al. (2016). Global impacts of the 1980s regime shift. *Global Change Biology*, *22*(2), 682–703. https://doi.org/10.1111/gcb.13106

Sabeerali, C. T., Rao, S. A., Ajayamohan, R. S., & Murtugudde, R. (2012). On the relationship between Indian summer monsoon withdrawal and Indo-Pacific SST anomalies before and after 1976/1977 climate shift. *Climate Dynamics*, *39*(3–4), 841–859. https://doi.org/10.1007/s00382-011-1269-9

Saikranthi, K., Narayana Rao, T., Rajeevan, M., & Vijaya Bhaskara Rao, S. (2013). Identification and validation of homogeneous rainfall zones in India using correlation analysis. *Journal of Hydrometeorology*, *14*(1), 304–317. https://doi.org/10.1175/JHM-D-12-071.1

Sarkar, S., & Maity, R. (2020a). Estimation of probable maximum precipitation in the context of climate change. *MethodsX*, *7*(100904), 1–8. https://doi.org/10.1016/j.mex.2020.100904

Sarkar, S., & Maity, R. (2020b). Increase in probable maximum precipitation in a changing climate over India. *Journal of Hydrology*, *585*, 124806. https://doi.org/10.1016/j.jhydrol.2020.124806

Sarkar, S., & Maity, R. (2021). Global climate shift in 1970s causes a significant worldwide increase in precipitation extremes. *Scientific Reports*, *11*(1), 1–12. https://doi.org/10.1038/s41598-021-90854-8

Sharma, S., & Mujumdar, P. (2017). Increasing frequency and spatial extent of concurrent meteorological droughts and heatwaves in India. *Scientific Reports*, *7*(1), 1–9. https://doi.org/10.1038/s41598-017-15896-3

Sharma, S., & Mujumdar, P. P. (2019). On the relationship of daily rainfall extremes and local mean temperature. *Journal of Hydrology*, *572*, 179–191. https://doi.org/10.1016/j.jhydrol.2019.02.048

Sillmann, J., Kharin, V. V., Zwiers, F. W., Zhang, X., & Bronaugh, D. (2013). Climate extremes indices in the CMIP5 multimodel ensemble: Part 2. Future climate projections. *Journal of Geophysical Research: Atmospheres*, *118*(6), 2473–2493. https://doi.org/10.1002/jgrd.50188

Singh, R., Jaiswal, N., & Kishtawal, C. M. (2022). Rising surface pressure over Tibetan Plateau strengthens Indian summer monsoon rainfall over northwestern India. *Scientific Reports*, *12*(1), 1–15. https://doi.org/10.1038/s41598-022-12523-8

Stegall, S. T., & Kunkel, K. E. (2019). Simulation of daily extreme precipitation over the United States in the CMIP5 30-Yr decadal prediction experiment. *Journal of Applied Meteorology and Climatology*, *58*(4), 875–886. https://doi.org/10.1175/JAMC-D-18-0057.1

Suman, M., & Maity, R. (2020). Southward shift of precipitation extremes over south Asia: Evidences from CORDEX data. *Scientific Reports*, *10*(1), 1–11. https://doi.org/10.1038/s41598-020-63571-x

Suman, M., Maity, R., & Kunstmann, H. (2021). Precipitation of Mainland India: Copula-based bias-corrected daily CORDEX climate data for both mean and extreme values. *Geoscience Data Journal*, *9*(1), 1–16. https://doi.org/10.1002/gdj3.118

Supharatid, S., Nafung, J., & Aribarg, T. (2021). Projected changes in temperature and precipitation over mainland Southeast Asia by CMIP6 models. *Journal of Water and Climate Change*, *13*, 1–20. https://doi.org/10.2166/wcc.2021.015

Taylor, K. E., Stouffer, R. J., & Meehl, G. A. (2012). An overview of CMIP5 and the experiment design. *Bulletin of the American Meteorological Society*, *93*(4), 485–498. https://doi.org/10.1175/BAMS-D-11-00094.1

Themeßl, M. J., Gobiet, A., & Leuprecht, A. (2011). Empirical-statistical downscaling and error correction of daily precipitation from regional climate models. *International Journal of Climatology*, *31*(10), 1530–1544. https://doi.org/10.1002/joc.2168

Trenberth, K. E. (2011). Changes in precipitation with climate change. *Climate Research*, *47*(1–2), 123–138. https://doi.org/10.3354/cr00953

Trenberth, K. E., Dai, A., Rasmussen, R. M., & Parsons, D. B. (2003). The changing character of precipitation. *Bulletin America Meteorology Social*, *84*, 1205–1217. https://doi.org/10.1175/BAMS-84-9-1205

Villarini, G., Smith, J. A., & Vecchi, G. A. (2013). Changing frequency of heavy rainfall over the central United States. *Journal of Climate*, *26*(1), 351–357. https://doi.org/10.1175/JCLI-D-12-00043.1

Wang, D., Liu, J., Shao, W., Mei, C., Su, X., & Wang, H. (2021). Comparison of CMIP5 and CMIP6 multi-model ensemble for precipitation downscaling results and observational data: The case of Hanjiang river basin. *Atmosphere*, *12*(7), 867. https://doi.org/10.3390/atmos12070867

Zheng, Y., Bourassa, M. A., Ali, M. M., & Krishnamurti, T. N. (2016). Distinctive features of rainfall over the Indian homogeneous rainfall regions between strong and weak Indian summer monsoons. *Journal of Geophysical Research: Atmospheres*, *121*(10), 5631–5647. https://doi.org/10.1002/2016JD025135

Zhou, T., Yu, R., Zhang, J., Drange, H., Cassou, C., Deser, C., et al. (2009). Why the western pacific subtropical high has extended Westward since the late 1970s. *Journal of Climate*, *22*(8), 2199–2215. https://doi.org/10.1175/2008JCLI2527.1

Zhou, X., Huang, G., Wang, X., & Cheng, G. (2018). Future changes in precipitation extremes over Canada: Driving factors and inherent mechanism. *Journal of Geophysical Research: Atmospheres*, *123*(11), 5783–5803. https://doi.org/10.1029/2017JD027735